

On the Outsized Importance of Learning Rates in Local Update Methods

Zachary Charles
Jakub Konečný
Google Research

ZACHCHARLES@GOOGLE.COM
KONKEY@GOOGLE.COM

Abstract

We study a family of algorithms, which we refer to as *local update* methods, that generalize many federated learning and meta-learning algorithms. We prove that for quadratic objectives, local update methods perform stochastic gradient descent on a *surrogate* loss function which we exactly characterize. We show that the choice of client learning rate controls the condition number of that surrogate loss, as well as the distance between the minimizers of the surrogate and true loss functions. We use this theory to derive novel convergence rates for federated averaging that showcase this trade-off between the condition number of the surrogate loss and its alignment with the true loss function. We validate our results empirically, showing that in communication-limited settings, proper learning rate tuning is often sufficient to reach near-optimal behavior. We also present a practical method for automatic learning rate decay in local update methods that helps reduce the need for learning rate tuning, and highlight its empirical performance on a variety of tasks and datasets.

Keywords: Local Update Methods, Local SGD, Federated Averaging, Federated Learning, Meta Learning, MAML

1. Introduction

Historically, machine learning was analyzed from a “centralized” perspective, in which a model is trained on a single central source of data. In recent years, there has been a shift away from centralized machine learning, due in part to the increase of user data and the increasing awareness of the risks to privacy that can accompany centralized data collection.

Federated learning (FL) (Kairouz et al., 2019) is a distributed framework for learning models without directly sharing user data. In this framework, heterogeneous clients all use their own data to perform local training. In the popular FedAvg algorithm (McMahan et al., 2017), the client models are then averaged at a central server, broadcast to a (possibly different) sample of clients, and the process is repeated. The core tenet is that instead of having clients share data, we instead share the results of *local updates* the clients perform on their own datasets using an optimization algorithm.

While there has been growing interest in FL in research communities (see (Kairouz et al., 2019) and (Li et al., 2019) for surveys of many recent works and open problems), this general paradigm of performing local updates on heterogeneous datasets has a storied history in machine learning. In particular, much of the work on meta-learning has focused on trying to learn models that perform well (or can quickly learn how to perform well) on a large number of heterogeneous tasks. This similarity with FL is even more clear in work on model-agnostic meta-learning (MAML) (Finn et al., 2017), in which local client gradient

updates are used to learn a global model. Connections between these two areas were noted by Jiang et al. (2019) and have since been explored in many other works (Khodak et al., 2019; Fallah et al., 2020).

While there is a wide variety of theoretical and empirical analyses of the aforementioned methods, it is generally difficult to understand their behavior in *heterogeneous settings*. There is enough evidence that these methods are useful in practice in complex scenarios (Hard et al., 2018; Yang et al., 2018; Hard et al., 2020), yet on a theoretical level, many works derive results comparable to, or worse than, that of mini-batch SGD in heterogeneous or even homogeneous settings; See (Kairouz et al., 2019) for a discussion of homogeneity and heterogeneity, and see (Woodworth et al., 2020) for a detailed discussion of comparisons to mini-batch SGD. Unfortunately, these results shed little light onto how methods such as FedAvg improve (or degrade) convergence.

In this work, we analyze a generalized local update paradigm that encompasses many FL and MAML methods, as well as other popular optimization methods such as mini-batch SGD. In order to better understand the structure of these methods in heterogeneous settings without an abundance of assumptions, we focus on the special case of quadratic loss functions. We are generally concerned with understanding the following questions that bridge both theory and practice.

- How do local update methods improve or hinder convergence?
- Why, despite a relative paucity of theoretical evidence, do these methods often perform better in practice than theoretically established methods such as mini-batch SGD?
- What obstacles are there to the performance of local update methods, and how do we mitigate these issues?

As a partial answer to these questions, we highlight the main findings of our work.

1. We show that in the quadratic case, local update methods are equivalent to the stochastic gradient method on a surrogate loss function which we exactly characterize. Thus, we can view local update methods that use multiple heterogeneous datasets as instead performing SGD on a single “central” loss function.
2. We show that methods such as FedAvg and many incarnations of MAML implicitly regularize the condition number of this surrogate loss function, allowing for improved convergence of the surrogate loss. On the other hand, we show that this condition number reduction comes at the cost of increasing the discrepancy between minimizers of the surrogate and the true loss function. Notably, this trade-off is controlled by fundamental algorithmic choices, especially the choice of learning rate.
3. We give explicit convergence rates for FedAvg that exhibit the trade-off between the condition number and the discrepancy between the surrogate and true loss functions above. Our results are similar in scope to work by Woodworth et al. (2020) (showing that local SGD can outperform mini-batch SGD), but work under heterogeneous data settings.

4. We use our theoretical insights to design practical improvements to federated learning methods. First, we show that *decoupling client and server learning rates* has significant implications for improving convergence to better models. We show that despite the non-optimality of critical points of FedAvg, combining this learning rate decoupling with proper tuning can result in near-optimal performance in settings with limited communication. Finally, we detail a simple, practical method for automatic learning rate decay in federated learning that helps reduce the burden of learning rate tuning. We show empirically that this method improves the convergence of FedAvg, without requiring manually crafted learning rate schedules, across a suite of realistic and challenging non-convex tasks.

1.1 Related work

Federated learning Federated learning is a distributed machine learning paradigm in which training is done locally on clients, without any centralized data aggregation. Federated learning has enabled privacy-aware learning in a variety of applications (Hard et al., 2018; Chen et al., 2019; Brisimi et al., 2018; Samarakoon et al., 2018; Hard et al., 2020), and has seen a large volume of work on the intersection of federated learning with topics including differential privacy (McMahan et al., 2018; Augenstein et al., 2020), fairness (Mohri et al., 2019; Li et al., 2020b), robustness (Ghosh et al., 2019; Bagdasaryan et al., 2018; Sun et al., 2019), and communication-efficiency (Konečný et al., 2016; Sattler et al., 2019; Basu et al., 2019; Reisizadeh et al., 2020). For a more detailed discussion of federated learning, we defer to surveys by Kairouz et al. (2019) and Li et al. (2019).

Meta-learning In meta-learning (aka *learning to learn*), the objective is to use a collection of tasks to learn how to learn a new task efficiently (Vanschoren, 2019). A particularly influential recent approach is model-agnostic meta-learning (MAML) proposed by Finn et al. (2017). The core idea has inspired a number of extensions (Antoniou et al., 2019; Nichol et al., 2018; Rusu et al., 2019; Grant et al., 2018; Rajeswaran et al., 2019; Raghu et al., 2020), which broadly use a two-level optimization structure to perform meta-learning. Convergence properties of some of these optimization algorithms were recently studied by Fallah et al. (2019), who also highlight differences in convergence of MAML and first-order approximations to MAML.

Federated optimization One of the most common approaches to optimization in the setting of federated learning is the FedAvg method (McMahan et al., 2017). While designed for heterogeneous sources of data, the study of FedAvg has roots in that of Local SGD (Zinkevich et al., 2010; Stich, 2019; Wang and Joshi, 2018; Stich and Karimireddy, 2019; Yu et al., 2019; Khaled et al., 2020), a communication-efficient optimization method for homogeneous clients. As interest in federated learning has grown, so too has the number of proposed federated optimization methods. These can often be seen as variants of FedAvg, that incorporate techniques such as momentum (Hsu et al., 2019), adaptive optimization (Reddi et al., 2020; Xie et al., 2019), proximal updates (Li et al., 2020a; Pathak and Wainwright, 2020) and control variates (Karimireddy et al., 2019). We again defer to Kairouz et al. (2019) and Li et al. (2019) for more detailed references.

Convergence (and non-convergence) of FedAvg While we defer to Kairouz et al. (2019, Section 3.2) for a complete discussion of federated optimization, we discuss a few important connections. First, while there has been huge progress in theoretical understandings of FedAvg, existing works generally have not been able to show that these methods consistently improve upon mini-batch SGD (Woodworth et al., 2020). Even theoretically and empirically successful techniques such as SCAFFOLD (Karimireddy et al., 2019) have only been shown to converge faster than mini-batch SGD on quadratic objectives.

This failure of convergence was noted by Li et al. (2020c), who showed that without learning rate decay, FedAvg is not guaranteed to converge. Later, Karimireddy et al. (2019) and Woodworth et al. (2020) showed that there are settings where FedAvg converges provably slower than mini-batch SGD. Similarly, Malinovsky et al. (2020) and Pathak and Wainwright (2020) showed that in heterogeneous settings, FedAvg can converge to sub-optimal points, even in non-stochastic, strongly convex settings. Pathak and Wainwright (2020) further give a proximal version of federated gradient descent that converges to the empirical risk minimizer in convex settings.

Comparisons to our work Our work is most closely related to that of Malinovsky et al. (2020), Pathak and Wainwright (2020). We also evince the non-convergence of FedAvg. However, we extend the analysis to stochastic settings, and to a more general class of algorithms that encompasses many meta-learning algorithms. As such, our work is also closely related to that of Fallah et al. (2019), who demonstrated differences (and non-convergence issues) of various MAML algorithms. Our work takes this a step further, where we give a unified view of both MAML and federated learning methods, and give a broader characterization of the sub-optimal convergence of these methods in the case of quadratic losses. Our work is also novel in its focus on the interplay between convergence, suboptimality, and algorithmic choices, especially learning rates.

Notation For a vector $v \in \mathbb{R}^d$, we let $\|v\|$ denote its ℓ_2 norm. For a matrix $A \in \mathbb{R}^{n \times m}$, we let $\|A\|$ denote its operator norm with respect to the ℓ_2 vector norm. For a symmetric positive semi-definite matrix A , we will let $A^{1/2}$ denote its matrix square root. For any real symmetric matrix A (therefore with real eigenvalues), we will let $\lambda_{\max}(A)$ and $\lambda_{\min}(A)$ denote its largest and smallest eigenvalues, respectively.

2. Preliminaries

Suppose we wish to learn a model $x \in \mathbb{R}^d$. Let \mathcal{I} denote some collection of *clients*, and let \mathcal{P} be a distribution on \mathcal{I} . For each $i \in \mathcal{I}$, we assume that there is an associated *data distribution* \mathcal{D}_i on some example space \mathcal{Z} . For any $z \in \mathcal{Z}$, we assume there is a unique corresponding symmetric matrix $A_z \in \mathbb{R}^{d \times d}$ and vector $c_z \in \mathbb{R}^d$, and define a quadratic loss function

$$f(x; z) := \frac{1}{2} \|A_z^{1/2}(x - c_z)\|^2. \quad (1)$$

We let $\nabla f(x; z)$ denote the gradient of the function $x \mapsto f(x; z)$ with respect to x . For $i \in \mathcal{I}$, we define the client loss function f_i and the overall loss function f as follows:

$$f_i(x) := \mathbb{E}_{z \sim \mathcal{D}_i} [f(x; z)], \quad f(x) := \mathbb{E}_{i \sim \mathcal{P}} [f_i(x)]. \quad (2)$$

One common objective in our setup is to minimize $f(x)$, though this is often not the direct goal of MAML methods. Note that the joint distribution over $(\mathcal{I}, \mathcal{Z})$ implicitly defines a (marginal) distribution over \mathcal{Z} , recovering standard risk minimization frameworks. This framework also encompasses distributed risk minimization in which \mathcal{P} is a uniform distribution over a finite set of nodes $i \in \mathcal{I}$ and \mathcal{D}_i is the uniform distribution over the (finite) dataset stored at node i . However, we take a more general approach and do not assume \mathcal{I} or \mathcal{Z} to be finite throughout. We also focus on the *heterogeneous* setting, where the client distributions \mathcal{D}_i are not all identical, as opposed to the *homogeneous* setting, where all \mathcal{D}_i are identical.

Modelling assumptions and relevance As FL has matured, it has become more evident that there are two varieties, with distinct system-imposed constraints, recently termed by Kairouz et al. (2019) as *cross-device federated learning* and *cross-silo federated learning*.¹ The primary distinction between these two frameworks that is relevant to our work is that in cross-silo FL, there are relatively few participating clients. Moreover, these clients are typically reliable and almost always available. By contrast, in cross-device FL there are potentially very large numbers of clients, only a small fraction of which are available at any given point in time. Furthermore, the clients cannot be addressed directly or re-identified if participating multiple times. For a more detailed summary, see (Kairouz et al., 2019, Table 1).

In cross-device FL, a client i sampled from \mathcal{I} corresponds to a single device, and \mathcal{D}_i corresponds to the data available on that device. In many practical cross-device FL systems (see Bonawitz et al. (2019); Hard et al. (2018)), the server does not control the selection of clients from the global population \mathcal{I} . Instead, participation is initiated by the clients, based on pre-defined eligibility criteria, such as whether the device is charging and on unmetered wifi. Thus, the client distribution \mathcal{P} can be considered as fixed, with only minor possibilities for it to be shaped by the server (e.g. whether to enforce sampling without replacement).

On the other hand, in many examples of cross-silo FL, participating clients correspond to various medical or financial organizations, or different geographical regions of the same organization (Wen et al., 2019; Yang et al., 2019). The participating clients are typically fixed in advance, and often all of them participate in every communication round. Thus, while cross-silo FL may be accurately described by a finite-sum optimization problem, this framework is less useful for cross-device FL.

To see this, consider the task of next word prediction on mobile devices. The FL training described by Hard et al. (2018) runs for 3000 communication rounds, with up to 500 clients participating in each round. That is at most 1.5 million distinct clients, a small fraction of the total number of possible clients². This also implies that it is nearly impossible to compute exact values of the loss $f(x)$. Instead, evaluation of a model’s quality is done using the same mechanism as the training – by using a subset of the clients eligible at a given time – which has significant implications for algorithm design (as we discuss in Sections 8 and 9). These issues are exacerbated by heterogeneity; Under extreme heterogeneity, finite-sum modelling approaches may lead to theory that does not accurately represent practical FL

1. A different categorization, *vertical* and *horizontal*, was proposed by Yang et al. (2019), which is based on modelling constraints, rather than on system constraints. The setup in this work applies primarily to horizontal FL, though we expect that much of our framework carries over to the vertical setting.

2. As of May 26, 2020, the Google Play Store reports “1,000,000,000+ installs” for the GBoard application.

systems. Thus, our modelling assumptions are designed to encompass both cross-silo and cross-device setting.

Our setup is also relevant to that of model-agnostic meta-learning (MAML), first proposed by Finn et al. (2017). In MAML, the main objective is to find a gradient-based mechanism, which given a task i sampled from \mathcal{P} , adapts to have good performance on the distribution \mathcal{D}_i . Unlike cross-device FL, where we generally cannot quantify \mathcal{P} directly because of data restrictions, the distribution \mathcal{P} is the primary object of interest in MAML. However, much like cross-device FL this distribution is generally not known a priori, but instead is problem-dependent.

2.1 LOCALUPDATE algorithms

In the following, we will consider a broad class of algorithms that attempt to minimize $f(x)$ (such as in FL methods) or attempt to learn a model that personalizes well with respect to \mathcal{P} (such as in meta learning algorithms). We refer to these as LOCALUPDATE algorithms. In such methods, at each round, a central coordinator (which we will refer to as a *server*) works with M *clients* (or in the language of MAML, tasks) sampled from \mathcal{P} and broadcasts its global model to the clients. Each client i optimizes its loss function f_i (initializing at the broadcast model) by iteratively applying mini-batch SGD with batch size B and *client* (inner) learning rate γ . The mini-batch gradients are computed by taking samples from the client’s local dataset \mathcal{D}_i . The client then sends a linear combination (parameterized by $\Theta = (\theta_1, \theta_2, \dots)$ where $\theta_i \in \mathbb{R}_{\geq 0}$) of its gradients to the server. We will only consider Θ with finite support. For such Θ , we define

$$K(\Theta) = \max\{i \mid \theta_i > 0\}.$$

Throughout our work, we will omit the trailing zeros in any Θ with finite support. The server averages the available updates, and, treating this average as a stochastic gradient of the loss function $f(x)$, performs a gradient step with a *server* (outer) learning rate η . Algorithms 1 and 2 give pseudo-code for LOCALUPDATE.

| Algorithm 1 LOCALUPDATE: Outer Loop | Algorithm 2 LOCALUPDATE: Inner loop |
|--|--|
| OuterLoop ($x, \{\eta_t\}_{t \geq 1}, \{\gamma_t\}_{t \geq 1}, \Theta$): $x_1 = x$ for each round $t = 1, 2, \dots, T$ do $I_t \leftarrow$ (random set of M clients) for each client $i \in I_t$ in parallel do $q_t^i \leftarrow$ InnerLoop(i, x_t, γ_t, Θ) $q_t \leftarrow (1/M) \sum_{i \in I_t} q_t^i$ $x_{t+1} = x_t - \eta_t q_t$ return x_{T+1} | InnerLoop (i, x, γ, Θ): $x_1 = x$ for $k = 1, 2, \dots, K(\Theta)$ do sample a set S_k of size B from \mathcal{D}_i $g_k = (1/B) \sum_{z \in S_k} \nabla f(x_k; z)$ $x_{k+1} \leftarrow x_k - \gamma g_k$ return $\sum_{k=1}^{K(\Theta)} \theta_k g_k$ |

This method recovers some well-known algorithms for specific choice of γ, η , and Θ . For convenience of notation, we define

$$\Theta_K = \underbrace{(0, \dots, 0)}_{K-1 \text{ times}}, 1, \tag{3}$$

so in particular $\Theta_1 = (1)$ and $K(\Theta_1) = 1$, and similarly

$$\Theta_{1:K} = \underbrace{(1, \dots, 1)}_{K \text{ times}}. \quad (4)$$

Many existing training algorithms can be expressed as special cases of LOCALUPDATE. We give a non-exhaustive list below.

- The simplest setting is mini-batch SGD. This can be recovered in multiple ways. For example, suppose each client i corresponds to a single example z_i . Then, LOCALUPDATE with $\Theta = \Theta_1$ is equivalent to mini-batch SGD with batch size M and learning rate η .
- Alternatively, if there is only a single client ($|\mathcal{I}| = 1$), then LOCALUPDATE with $\Theta = \Theta_1$ becomes mini-batch SGD with batch size B and learning rate η . As expected, the choice of γ has no impact in either instance of mini-batch SGD.
- More generally, setting $\Theta = \Theta_1$ recovers distributed mini-batch SGD, with total batch size MB and learning rate η . Again, γ has no impact on the global model.
- When there is a single client and $\Theta = \Theta_{1:K}$, then LOCALUPDATE recovers the Lookahead optimizer (Zhang et al., 2019) with K “fast weights”.
- In the homogeneous setting, if $\Theta = \Theta_{1:K}$, and $\gamma = \eta$, then LOCALUPDATE is equivalent to Local SGD with K local steps. For further details, see Appendix A.
- In the heterogeneous setting, if we set $\Theta = \Theta_{1:K}$ and $\gamma = \eta$, then LOCALUPDATE is equivalent to FedAvg with K local steps (see Appendix A for details). When γ and η are not necessarily equal, we actually recover Reptile (Nichol et al., 2018), as well as the Generalized FedAvg algorithm in (Reddi et al., 2020). For convenience of notation, we will refer to this algorithm as FedAvg/Reptile throughout. This equivalence between FedAvg and Reptile was first noted by Jiang et al. (2019). In fact, we show in Section 8 that this decoupling of client and server learning rates is critical to understanding and improving the convergence of FedAvg.
- When $\Theta = \Theta_K$, we recover the first-order MAML (FOMAML) algorithm of Finn et al. (2017). A similar functional relation between FOMAML and Reptile was previously described by Nichol et al. (2018).
- In the MAML algorithm, Finn et al. (2017) use K local update steps for each “task” (in our vocabulary, client). We will refer to this as \mathcal{K} -MAML throughout. As we show in Section 3.1, when the underlying loss functions are quadratic and the clients perform gradient descent updates, \mathcal{K} -MAML is recovered by setting $\Theta = \Theta_{2K+1}$. This gives a previously unknown connection between FL and MAML algorithms. As we discuss in Section 3.1, this does not hold when the clients use SGD due to potential biases in estimating Hessian-gradient products via stochastic gradients.

As written, both clients and server use SGD as their optimizer in LOCALUPDATE. However, one could use techniques such as momentum or adaptive learning rates on either the

server (as explored by Reddi et al. (2020)) or the client (as explored by Xie et al. (2019)). While our results can be extended to these settings, we leave this to future work. Our goal is not to derive convergence results for as broad a class of algorithms as possible. Rather, we wish to understand how the choice of γ and Θ impact the dynamics of optimization, especially in heterogeneous settings.

We note that in Algorithm 2, each client performs a designated number of steps of mini-batch SGD, with samples taken from some underlying client distribution \mathcal{D}_i . When \mathcal{D}_i is the uniform distribution over some finite set \mathcal{S}_i , we could instead write Algorithm 2 in terms of performing some number of epochs E of mini-batch SGD over \mathcal{S}_i , as is done in (McMahan et al., 2017) and many other works on federated learning. In this case, the batch size B dictates the number of client gradient steps (as the client roughly take $E|\mathcal{S}_i|/B$ steps). Thus, in such settings, the choice of B has an analogous impact as the choice of the number of local steps $K(\Theta)$ in Algorithm 2. For simplicity of analysis, we will analyze the latter throughout, but our results can be easily extended to the former.

2.2 Outline

The rest of this paper is organized as follows. In Section 3, we show that a round of LOCALUPDATE method is equivalent to performing a *single* (stochastic) gradient step with respect to a surrogate objective, which we exactly characterize.

In Section 4, we use simple examples to show that the surrogate loss and the original loss can vary substantially. Moreover, we show how choices of γ and Θ affect the discrepancy between the two losses. In particular, we highlight how the choice of γ is crucial to the performance of LOCALUPDATE. In Section 5, we analyze spectral properties of the surrogate loss, and show that LOCALUPDATE can be viewed as implicit regularization on the condition number, where the amount of regularization is controlled by γ and Θ .

The next sections present to the best of our knowledge a novel proof technique, characterizing the convergence of FedAvg/Reptile in heterogeneous settings.³ In Section 6, we bound the distance between the minimizers of the surrogate and the true loss function in terms of the client learning rate γ . We use these results in Section 7 to derive convergence rates for FedAvg/Reptile that highlight how the choice of client learning rate γ gives rise to a trade-off between local and global optimization. In particular, we show that learning rate decay is both sufficient and necessary for convergence to the true risk minimizer.

While our theoretical results are valid only for quadratic loss functions, in Section 8 we show empirically that our conclusions carry over to more general settings, including non-convex objectives. Our empirical results highlight the importance of learning rate tuning in federated learning. In Section 9, we combine our theoretical insights with important systems-level constraints to design a method for automatic learning rate decay methods for local update methods. In particular, we present a simple, easy to implement method for automatic learning rate decay, and show its efficacy in improving accuracy and reducing the need for client learning rate tuning.

3. While we focus on FedAvg and Reptile, we note that a similar analysis can be performed for any of the special cases listed above, using a similar proof strategy.

3. LOCALUPDATE as SGD

When $K(\Theta) > 1$ and $\gamma > 0$, the dynamics of LOCALUPDATE may be very different than those of mini-batch SGD. We will show that for quadratic functions, these dynamics are related but distinct. In particular, we will show that any local update method on a quadratic function can be viewed as SGD on some appropriately defined surrogate loss function. Moreover, the discrepancy between the true loss function and the surrogate loss function is dictated by the choice of client learning rate γ and Θ .

For $i \in \mathcal{I}$, define:

$$A_i := \mathbb{E}_{z \sim \mathcal{D}_i} [A_z].$$

We assume throughout that A_i is finite and invertible. We also define

$$c_i := A_i^{-1} \mathbb{E}_{z \sim \mathcal{D}_i} [A_z c_z].$$

Again, we assume this is finite. We then have the following lemma.

Lemma 1 *For all $i \in \mathcal{I}$, there is some constant τ_i such that*

$$f_i(x) = \frac{1}{2} \|A_i^{1/2}(x - c_i)\|^2 + \tau_i.$$

In the sequel, we will omit the constant term τ_i , and let

$$f_i(x) = \frac{1}{2} \|A_i^{1/2}(x - c_i)\|^2$$

as this does not change the gradients of the loss f_i . Since each A_z is symmetric and positive definite, so is A_i . We define the following:

$$A := \mathbb{E}_{i \sim \mathcal{P}} [A_i], \quad c := \mathbb{E}_{i \sim \mathcal{P}} [c_i].$$

We will assume that these expectations exist and are finite throughout. We will also utilize the following mild assumptions at different times.

Assumption 1 $K(\Theta) > 0$.

Assumption 2 *There are $\mu, L > 0$ such that for all i ,*

$$\mu I \preceq A_i \preceq LI.$$

Assumption 3 *There are finite σ_A and σ_c such that*

$$\mathbb{E}_{i \sim \mathcal{P}} [\|A_i - A\|^2] \leq \sigma_A^2.$$

$$\mathbb{E}_{i \sim \mathcal{P}} [\|c_i - c\|^2] \leq \sigma_c^2.$$

Assumption 1 prevents pathologically bad choices of Θ in which clients simply send 0 to the server at every round. Assumption 2 amounts to assuming upper and lower bounds on the Lipschitz and strong convexity parameters of each loss function f_i . This is satisfied if there are a finite number of clients, and for each, A_i is positive definite. However, it is often true in more generality if the underlying matrices A_z satisfy some kind of bounded eigenvalue condition. Moreover, when the number of clients is finite, we can always ensure that $\mu I \preceq A_i$ for all i by adding ℓ_2 regularization to our objective function.

Assumption 3 assumes that the matrices A_i and optimal points c_i for each loss function have bounded variance. We do not assume that the gradients computed by the clients have bounded norm. Intuitively, as $\sigma_c \rightarrow 0$, local update methods should provide more benefit, as the clients are taking more steps towards a shared optimum. While $\sigma_c = 0$ in the case of homogeneous data distributions (i.e. \mathcal{D}_i are the same for all $i \in \mathcal{I}$), these two conditions are not equivalent. There are heterogeneous data distributions which still yield $\sigma_c = 0$. Also, note that c is in general not the minimizer of the objective f .

Fix $i \in \mathcal{I}$, and consider Algorithm 2. We initialize $x_1 = x$, and then at each iteration k we sample a set S_k uniformly at random (with replacement) from \mathcal{D}_i , then update via

$$g_k = \frac{1}{B} \sum_{z \in S_k} \nabla f(x_k; z), \quad (5)$$

$$x_{k+1} = x_k - \gamma g_k. \quad (6)$$

We first prove a basic recurrence relation concerning the local gradients g_k for task i .

Lemma 2 *For $i \in \mathcal{I}$, suppose that A_i is invertible and g_k as in Algorithm 2, for all $k \geq 1$,*

$$\mathbb{E}[g_{k+1}] = (I - \gamma A_i) \mathbb{E}[g_k]. \quad (7)$$

Defining the surrogate loss Using Lemma 2, we will show that Algorithm 2 can be viewed as performing SGD on a *surrogate loss*. This surrogate loss will be parameterized by the inputs γ and Θ to Algorithm 2. To define the surrogate loss, we first define, for each client $i \in \mathcal{I}$, a *distortion matrix* $Q_i(\gamma, \Theta)$ as follows:

$$Q_i(\gamma, \Theta) := \sum_{k=1}^{K(\theta)} \theta_k (I - \gamma A_i)^{k-1}. \quad (8)$$

We can then define, for each $i \in \mathcal{I}$, the client's surrogate loss function:

$$\tilde{f}_i(x, \gamma, \Theta) := \frac{1}{2} \|(Q_i(\gamma, \Theta) A_i)^{1/2} (x - c_i)\|. \quad (9)$$

The overall surrogate loss function is then given by

$$\tilde{f}(x, \gamma, \Theta) := \mathbb{E}_{i \sim \mathcal{P}} [\tilde{f}_i(x, \gamma, \Theta)]. \quad (10)$$

Informally, the matrix $Q_i(\gamma, \Theta)$ can be viewed as causing a distortion to the matrix A_i . When $\Theta = \Theta_1$, one can see that $Q_i(\gamma, \Theta) = I$, in which case there is no distortion. For other Θ , $Q_i(\gamma, \Theta)$ may significantly distort A_i , and can amplify heterogeneity of the A_i . Using Lemma 2, we derive the following property of the output of the Algorithm 2.

Theorem 3 *Suppose that A_i is invertible. Then*

$$\mathbb{E}[\text{InnerLoop}(i, x, \gamma, \Theta)] = \nabla_x \tilde{f}_i(x, \gamma, \Theta) = Q_i(\gamma, \Theta) \nabla f_i(x). \quad (11)$$

Proof By direct computation,

$$\nabla \tilde{f}_i(x, \gamma, \Theta) = Q_i(\gamma, \Theta) A_i(x - c_i).$$

On the other hand, by Lemma 2,

$$\begin{aligned} \mathbb{E}[\text{InnerLoop}(i, w, \gamma, \Theta)] &= \sum_{k=1}^{K(\theta)} \theta_k (1 - \gamma A_i)^{k-1} \mathbb{E}[g_1] \\ &= \sum_{k=1}^{K(\theta)} \theta_k (1 - \gamma A_i)^{k-1} A_i(x - c_i) \\ &= Q_i(\gamma, \Theta) A_i(x - c_i). \end{aligned}$$

This proves the first equality. The second follows from noting that $\nabla f_i(x) = A_i(x - c_i)$. ■

Let q_t be as in Algorithm 1. Then Theorem 3 implies $\mathbb{E}[q_t] = \nabla \tilde{f}(x, \gamma, \Theta)$. In particular, one round of LOCALUPDATE with a given γ, Θ is equivalent to performing one step of SGD on the surrogate loss function $\tilde{f}(x, \gamma, \Theta)$.

We note that a version of Theorem was first shown for the case $\Theta = \Theta_2$ by Fallah et al. (2020), and was used to compare the behavior of FOMAML and MAML. We will take this comparison a step further, by showing in Section 3.1 that in the non-stochastic client setting, MAML can also be viewed as performing SGD on a similarly-defined surrogate loss.

Theorem 3 has important consequences regarding the impact of other “outer optimizers” in Algorithm 1, such as the adaptive server optimization (Reddi et al., 2020). If we treat the the output of Algorithm 2 simply as a stochastic gradient oracle of $\tilde{f}(x, \gamma, \Theta)$, we can apply existing convergence guarantees of any gradient based methods to understand the behavior of LOCALUPDATE method with different outer optimizers. In particular, this implies that the choice of outer optimization method primarily impacts the *speed* of convergence to $\text{argmin}_x \tilde{f}(x, \gamma, \Theta)$, but not the point LOCALUPDATE actually converges to. We empirically analyze the use of adaptive server methods in LOCALUPDATE in Sections 8 and 9.

3.1 MAML

As previously discussed, in the setting above, one can actually view MAML as a special case of LOCALUPDATE. In this section we elaborate on the claim, using a similar presentation of MAML as in (Nichol et al., 2018). MAML with K local steps (which we refer to as \mathcal{K} -MAML) can be viewed as a simple modification of LOCALUPDATE. Algorithm 1 proceeds in the same manner. In Algorithm 2, each client still executes K mini-batch SGD steps. However, what each client sends to the server differs from Algorithm 1.

For simplicity, we define $X_K^i(x)$ as the function that runs K steps of mini-batch SGD, starting from x , for some fixed mini-batches S_1, \dots, S_K of size B drawn independently from \mathcal{D}_i . For convenience, we let $X_0^i(x) = x$. We then define

$$m_K^i(x; z) := f(X_K^i(x); z), \quad (12)$$

$$m_K^i(x) := \mathbb{E}_{z \sim \mathcal{D}_i} m_K^i(x; z). \quad (13)$$

Note that these are implicitly functions of the mini-batches S_1, \dots, S_K sampled from \mathcal{D}_i . The output $q^i(x)$ of client i (as a function of its initial model x) is a stochastic estimate of $\nabla m_K^i(x)$, so that

$$\mathbb{E}[q^i(x)] = \nabla m_K(x; z), \quad (14)$$

The remainder of the MAML algorithm proceeds in the same way as LOCALUPDATE. Namely, the server averages the client outputs, and uses this as a gradient estimate with learning rate η . That is,

$$q(x) = \sum_{i \in I} q^i(x), \quad (15)$$

$$x' = x - \eta q(x). \quad (16)$$

We now show that when the clients use gradient descent to perform their local update, \mathcal{K} -MAML is in expectation equivalent to performing LOCALUPDATE with $\Theta = \Theta_{2K+1}$.

Theorem 4 *If $X_K^i(x)$ is the function that runs K steps of gradient descent, starting from x , on the client dataset \mathcal{D}_i , then*

$$\nabla m_K^i(x) = \mathbb{E}[\text{InnerLoop}(x, \gamma, \Theta_{2K+1})] = \nabla_x \tilde{f}_i(x, \gamma, \Theta_{2K+1}).$$

It is fruitful to reflect on what this means. Informally, this result shows that for quadratic functions, the gradient of the loss after K steps of gradient descent, taken with respect to the initial point x , is in expectation the gradient of the loss function after $K + 1$ additional SGD steps. In particular, given $q(x)$ as in (14), we have

$$\mathbb{E}[q(x)] = \nabla_x \tilde{f}(x, \gamma, \Theta_{2K+1}).$$

Thus, the MAML update in (16) amounts to a single stochastic gradient update on the surrogate loss function $\tilde{f}(x, \gamma, \Theta_{2K+1})$.

We note that this result relied on the clients using gradient descent to compute $X_k^i(x)$. For computational efficiency, this is often instead done using mini-batch SGD. However, computing $\nabla m_K^i(x)$ then involves computing unbiased estimates of the Hessian and gradient using the same batches of data. By the chain rule, estimating $\nabla m_K^i(x)$ involves multiplying these Hessian and gradient estimates. However, the product of these unbiased estimators need not be unbiased since they were computed with respect to the same batch of data. Thus, this correspondence between \mathcal{K} -MAML and LOCALUPDATE may break down in computationally-efficient (but biased) MAML implementations. For more detailed discussion on this bias, see (Fallah et al., 2019). We also note that Fallah et al. (2019) analyze the convergence properties of MAML and FOMAML, and independently observe that MAML and FOMAML need not share stationary points for quadratic objectives.

4. Local update methods tend towards different global minima

As we will show in Section 5, $\tilde{f}_i(x, \gamma, \Theta)$ shares many properties with $f_i(x)$, including having the same global minima. However, we first highlight that a crucial correspondence breaks down when considering the population-level global minima in heterogeneous settings. That is, in general

$$\operatorname{argmin}_x f(x) \neq \operatorname{argmin}_x \tilde{f}(x, \gamma, \Theta).$$

In order to enhance our understanding of the surrogate loss function, we first give both analytic and empirical examples.

Analytic examples Let \mathcal{P} have support $\{1, 2\}$, with each option equally likely. Suppose that $\mathcal{D}_1, \mathcal{D}_2$ have support only on the points $z = 1$ and $z = 2$ respectively, and suppose $A_z = z, c_z = 1/z$, so that $f(x; z) = \frac{1}{2}z(x - 1/z)^2$. We see that $f(x)$ is minimized at $x = 2/3$. On the other hand, let $\Theta = \Theta_{1:2}$. For $\gamma \geq 0$, we can compute the i -th distortion matrix by

$$Q_i(\gamma, \Theta) = 1 + (1 - \gamma i) = 2 - \gamma i.$$

Note that this is positive definite for $i = 1, 2$ as long as $\gamma \in [0, 1/2)$. By (10),

$$\tilde{f}(x, \gamma, \Theta) = \frac{(2 - \gamma)(x - 1)^2}{4} + (1 - \gamma)(x - 1/2)^2.$$

For $\gamma \in [0, 6/5)$, this is a positive definite quadratic function, with minimum given by

$$\operatorname{argmin}_x \tilde{f}(x, \gamma, \Theta) = \frac{4 - 3\gamma}{6 - 5\gamma},$$

implying

$$\|\operatorname{argmin}_x \tilde{f}(x, \gamma, \Theta) - \operatorname{argmin}_x f(x)\| = \frac{\gamma}{3(6 - 5\gamma)}.$$

Therefore, even if we run LOCALUPDATE until convergence, it would not converge to the true risk minimizer. This holds even though there are only two clients, each with a single data point. In other words, some form of learning rate decay is *necessary* for convergence to the risk minimizer. The necessity of learning rate decay was first shown by Li et al. (2020c), and later shown in (Malinovsky et al., 2020) and (Pathak and Wainwright, 2020). We take this analysis further, by showing how this sub-optimal behavior is explicitly governed by algorithmic choices, especially learning rate and the number of local steps taken.

For instance, in the example above, as $\gamma \rightarrow 0$, the surrogate risk minimizer converges to the true risk minimizer. Conversely, as γ increases, the two minima become further apart. In fact, as $\gamma \rightarrow 6/5$, the distance between the two optima grows arbitrarily large, even though $\tilde{f}(x, \gamma, \Theta)$ is a positive definite quadratic function. The critical issue here is that while $\gamma < 6/5$ ensures that $f(x, \gamma, \Theta_{1:2})$ is well-behaved (ie. that it is a positive definite quadratic function), it is not small enough to ensure that each client's surrogate loss function $\tilde{f}_i(x, \gamma, \Theta)$ is well-behaved. Note $f_2(x, \gamma, \Theta_{1:2})$ is a negative definite quadratic function for $\gamma > 1/2$, which causes this divergence. Even though the iterates of LOCALUPDATE are converging, there may be some client which is not converging in any meaningful sense. Therefore:

The client learning rate should be set sufficiently small so that all client loss functions are well-behaved, even if the overall loss function is well-behaved.

A similar analysis shows that if we instead fix γ , the distance between the surrogate risk and true risk minimizers depends on K . Let $\gamma = 1/2$. By (8),

$$Q_1(1/2, \Theta_{1:K}) = \sum_{k=0}^{K-1} 2^{-k} = 2 - 2^{-(K-1)}, \quad Q_2(1/2, \Theta_{1:K}) = 1,$$

implying

$$f(x, 1/2, \Theta_{1:K}) = \frac{1}{2} ((1 - 2^{-K})(x - 1)^2 + (x - 1/2)^2).$$

This is a positive definite quadratic with minima given by

$$\operatorname{argmin}_x f(x, 1/2, \Theta_{1:K}) = \frac{3 \cdot 2^K - 2}{2^{K+2} - 2}.$$

This then implies

$$\|\operatorname{argmin}_x f(x, 1/2, \Theta_{1:K}) - \operatorname{argmin}_x f(x)\| = \frac{2^K - 2}{6(2^{K+1} - 1)}.$$

When $K = 1$, this gap is 0, while as $K \rightarrow \infty$, the distance increases monotonically to $1/12$. In fact, as $K \rightarrow \infty$, the minimizer of the surrogate loss function converges to the expected value of the client loss minimizers. In Lemma 15 we prove an even stronger statement, and show that it holds for all positive definite quadratic loss functions.

Empirical examples Next, we give an empirical generalization of the above example for further illustration. Let $f(x; z) = (1/2)zx^2 - x$ for $z > 0$ (ie. $A_z = z$ and $c_z = 1/z$). We let \mathcal{P} have support $[0.5, 2]$ and density function $q(i) = 8i/15$. For each $i \in \operatorname{supp}(\mathcal{P})$, we let the client distribution \mathcal{D}_i be supported on a single point $z = i$, so that $f_i(x) = (1/2)ix^2 - x$. Again, deterministic f_i will still be sufficient observe discrepancies between the true and surrogate loss functions.

In Figure 1, we plot the behavior of FedAvg/Reptile with K local steps (LOCALUPDATE with $\Theta = \Theta_{1:K}$) on this problem. We fix $\eta = 10^{-4}$, $M = B = 1$, and illustrate the change in behavior as either γ varies and K is fixed, or K varies and γ is fixed. We also plot the true minimizer and the average minimizer, $\mathbb{E}_{i \sim \mathcal{P}}[\operatorname{argmin}_x f_i(x)]$.

If $\gamma = 0$ or $K = 1$, we converge to x^* . As γ or K increases, we converge to a point further from x^* . As $K \rightarrow \infty$ we converge to the average minimizer. We also see that *decreasing* the local stepsize *increases* the variance. This is to be expected: When $\gamma = 0$, LOCALUPDATE with $M = 1$ reduces to mini-batch SGD with batch size K , but the gradients in the batch are *summed* rather than averaged. For $\gamma > 0$, the magnitude of the gradients being summed decreases as the client converges to its minimizer. If we set γ to be larger than 1.0, we see an even greater gap between the surrogate minimizer and the true minimizer (due to the presence of negative-definite clients).

In Section 6, we derive general bounds on the distance between surrogate and true minimizers. To do so, we will use spectral properties of the matrix $Q_i(\gamma, \Theta)$, which we derive in the next section.

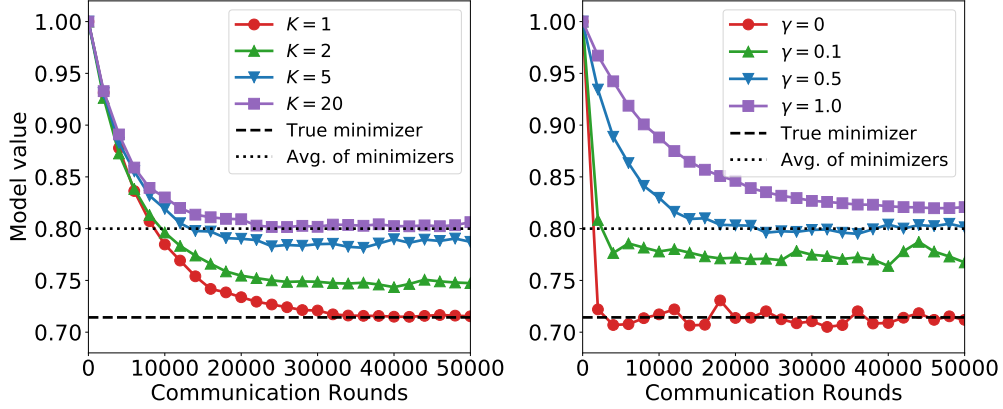


Figure 1: LOCALUPDATE convergence behavior with $\Theta = \Theta_{1:K}$ on an example 1-dimensional problem. (Left) We fix $\gamma = 0.5$ and vary K . (Right) We fix $K = 20$ and vary γ .

5. Surrogate loss properties

In order to understand the surrogate loss function $\tilde{f}(x, \gamma, \Theta)$, we will analyze properties of the distortion matrix $Q_i(\gamma, \Theta)$. We first note that in certain special cases, $Q_i(\gamma, \Theta)$ is some scaled version of the identity matrix. The following result is a simple consequence of the definition in (8).

Lemma 5 *Let $a = \sum_{k=1}^{K(\Theta)} \theta_k$. If $\gamma = 0$ or $K(\Theta) = 1$, then $Q_i(\gamma, \Theta) = aI$ and $\tilde{f}_i(x, \gamma, \Theta) = af_i(x)$.*

Under these settings, we therefore have $\tilde{f}(x, \gamma, \Theta) = af(x)$, and so the surrogate and true loss functions only differ by a constant. More generally, the functions $\tilde{f}_i(x, \gamma, \Theta)$ inherit many properties from $f_i(x)$, as captured in the following lemma.

Lemma 6 *Let $L_i = \lambda_{\max}(A_i)$, $\mu_i = \lambda_{\min}(A_i) > 0$ and suppose that $\gamma < L_i^{-1}$. Then*

1. $Q_i(\gamma, \Theta)$ is symmetric and positive definite.
2. $\tilde{f}_i(x, \gamma, \Theta)$ and $f_i(x)$ have the same unique global minimizer $x^* = c_i$.
3. For each eigenvalue λ of A_i , Q_i has an eigenvalue

$$\sum_{k=1}^{K(\Theta)} \theta_k (1 - \gamma \lambda)^{k-1}.$$

with the same multiplicity.

4. $Q_i(\gamma, \Theta)$ satisfies

$$\lambda_{\max}(Q_i(\gamma, \Theta)) = \sum_{k=1}^{K(\Theta)} \theta_k (1 - \gamma \mu_i)^{k-1}.$$

$$\lambda_{\min}(Q_i(\gamma, \Theta)) = \sum_{k=1}^{K(\Theta)} \theta_k (1 - \gamma L_i)^{k-1}.$$

For convenience, we note some special cases of Lemma 6 for $\Theta = \Theta_K, \Theta_{1:K}$.

Lemma 7 *Let $L_i = \lambda_{\max}(A_i), \mu_i = \lambda_{\min}(A_i)$ and suppose that $\gamma < L_i^{-1}$. Then*

$$\lambda_{\max}(Q_i(\gamma, \Theta_K)) = (1 - \gamma \mu_i)^K, \quad \lambda_{\min}(Q_i(\gamma, \Theta_K)) = (1 - \gamma L_i)^K.$$

If Assumption 2 holds and $\gamma < L^{-1}$, then

$$\lambda_{\max}(Q_i(\gamma, \Theta_K)) \leq (1 - \gamma \mu)^K, \quad \lambda_{\min}(Q_i(\gamma, \Theta_K)) \geq (1 - \gamma L)^K.$$

Lemma 8 *Let $L_i = \lambda_{\max}(A_i), \mu_i = \lambda_{\min}(A_i)$ and suppose that $\gamma < L_i^{-1}$. Then*

$$\lambda_{\max}(Q_i(\gamma, \Theta_{1:K})) = \frac{(1 - (1 - \gamma \mu_i)^K)}{\gamma \mu_i}, \quad \lambda_{\min}(Q_i(\gamma, \Theta_{1:K})) = \frac{(1 - (1 - \gamma L_i)^K)}{\gamma L_i}.$$

If Assumption 2 holds and $\gamma < L^{-1}$, then

$$\lambda_{\max}(Q_i(\gamma, \Theta_{1:K})) \leq \frac{(1 - (1 - \gamma \mu)^K)}{\gamma \mu}, \quad \lambda_{\min}(Q_i(\gamma, \Theta_{1:K})) \geq \frac{(1 - (1 - \gamma L)^K)}{\gamma L}.$$

As the eigenvalue bounds above suggest, $Q_i(\gamma, \Theta_{1:K})$ actually has a relatively simple form, as we show in the next lemma.

Lemma 9 *Suppose $0 < \gamma < L_i^{-1}$. Then*

$$Q_i(\gamma, \Theta_{1:K}) = (I - (I - \gamma A_i))(\gamma A_i)^{-1}.$$

Note that when $\gamma = 0$, (8) implies $Q_i(\gamma, \Theta_{1:K}) = KI$.

We are also interested in the matrix $Q_i(\gamma, \Theta)A_i$, as its eigenvalues govern the Lipschitz and strong convexity parameters of the function $\tilde{f}_i(x, \gamma, \Theta)$. We have the following result.

Lemma 10 *Let $L_i = \lambda_{\max}(A_i), \mu_i = \lambda_{\min}(A_i)$.*

1. *For each eigenvector and eigenvalue pair (v, λ) of A_i , v is an eigenvector of $Q_i(\gamma, \Theta)A_i$ with eigenvalue*

$$\sum_{k=1}^{K(\Theta)} \theta_k (1 - \gamma \lambda)^{k-1} \lambda.$$

2. *If $\gamma < L_i^{-1}$, $Q_i(\gamma, \Theta)A_i$ is symmetric and positive definite with eigenvalues satisfying*

$$\lambda_{\max}(Q_i(\gamma, \Theta)A_i) \leq \sum_{k=1}^{K(\Theta)} \theta_k (1 - \gamma \mu_i)^{k-1} L_i.$$

$$\lambda_{\min}(Q_i(\gamma, \Theta)A_i) \geq \sum_{k=1}^{K(\Theta)} \theta_k (1 - \gamma L_i)^{k-1} \mu_i.$$

The bounds in Lemma 10 can be refined for specific Θ . We first consider FedAvg/Reptile, when $\Theta = \Theta_{1:K}$. By Lemma 9, when $0 < \gamma < L_i^{-1}$, we have

$$Q_i(\gamma, \Theta_{1:K})A_i = \frac{I - (I - \gamma A_i)^K}{\gamma}.$$

We will therefore be able to compute the eigenvalues of $Q_i(\gamma, \Theta_{1:K})A_i$ in terms of the function

$$\phi_{K,\lambda}(\gamma) := \gamma^{-1}(1 - (1 - \gamma\lambda)^K). \quad (17)$$

In fact, $\phi_{K,\lambda}(\gamma)$ is actually continuous at 0, with its value being given by $\phi_{K,\lambda}(0) = K\lambda$. One way to see this is by noting that by basic properties of geometric sums, for $0 \leq \gamma \leq \lambda^{-1}$,

$$\phi_{K,\lambda}(\gamma) = \sum_{k=1}^K (1 - \gamma\lambda)^{k-1} \lambda. \quad (18)$$

We can now give strong bounds on the spectrum of $Q_i(\gamma, \Theta_{1:K})A_i$. We get the following:

Lemma 11 *Let $L_i = \lambda_{\max}(A_i)$, $\mu_i = \lambda_{\min}(A_i)$.*

1. *For each eigenvector, eigenvalue pair (v, λ) of A_i , v is an eigenvector of $Q_i(\gamma, \Theta_{1:K})A_i$ with eigenvalue $\phi_{K,\lambda}(\gamma)$.*
2. *If $\gamma < L_i^{-1}$, the maximum and minimum eigenvalues of $Q_i(\gamma, \Theta_{1:K})A_i$ are given by*

$$\lambda_{\max}(Q_i(\gamma, \Theta_{1:K})A_i) = \phi_{K,L_i}(\gamma),$$

$$\lambda_{\min}(Q_i(\gamma, \Theta_{1:K})A_i) = \phi_{K,\mu_i}(\gamma).$$

3. *If Assumption 2 holds and $\gamma < L^{-1}$, then*

$$\lambda_{\max}(Q_i(\gamma, \Theta_{1:K})A_i) \leq \phi_{K,L}(\gamma),$$

$$\lambda_{\min}(Q_i(\gamma, \Theta_{1:K})A_i) \geq \phi_{K,\mu}(\gamma).$$

We can also tighten the bounds in Lemma 10 for the MAML-style algorithms, where $\Theta = \Theta_K$, as long as the learning rate is set appropriately.

Lemma 12 *Let $L_i = \lambda_{\max}(A_i)$, $\mu_i = \lambda_{\min}(A_i)$.*

1. *For each eigenvector, eigenvalue pair (v, λ) of A_i , v is an eigenvector of $Q_i(\gamma, \Theta_K)A_i$ with eigenvalue $(1 - \gamma\lambda)^{K-1}\lambda$.*
2. *If $\gamma < (KL_i)^{-1}$, the maximum and minimum eigenvalues of $Q_i(\gamma, \Theta_K)A_i$ are given by*

$$\lambda_{\max}(Q_i(\gamma, \Theta_K)A_i) = (1 - \gamma L)^{K-1} L,$$

$$\lambda_{\min}(Q_i(\gamma, \Theta_K)A_i) = (1 - \gamma \mu)^{K-1} \mu.$$

3. If Assumption 2 holds and $\gamma < (KL)^{-1}$, then

$$\begin{aligned}\lambda_{\max}(Q_i(\gamma, \Theta_K)A_i) &\leq (1 - \gamma L)^{K-1}L, \\ \lambda_{\min}(Q_i(\gamma, \Theta_K)A_i) &\geq (1 - \gamma\mu)^{K-1}\mu.\end{aligned}$$

Lemmas 11 and 12 imply the following results regarding the condition number of the surrogate loss.

Corollary 13 *If Assumption 2 holds and $\gamma < L^{-1}$, then $\tilde{f}(x, \gamma, \Theta_{1:K})$ is \tilde{L} -smooth and $\tilde{\mu}$ -strongly convex where*

$$\begin{aligned}\tilde{L} &\leq \phi_{K,L}(\gamma), \\ \tilde{\mu} &\geq \phi_{K,\mu}(\gamma).\end{aligned}$$

Therefore, $\tilde{f}(x, \gamma, \Theta_{1:K})$ has condition number $\tilde{\kappa}$ satisfying

$$\tilde{\kappa} \leq \frac{\phi_{K,L}(\gamma)}{\phi_{K,\mu}(\gamma)} = \frac{1 - (1 - \gamma L)^K}{1 - (1 - \gamma\mu)^K}.$$

Corollary 14 *If Assumption 2 holds and $\gamma < (KL)^{-1}$, then $\tilde{f}(x, \gamma, \Theta_K)$ is \tilde{L} -smooth and $\tilde{\mu}$ -strongly convex where*

$$\begin{aligned}\tilde{L} &\leq (1 - \gamma L)^{K-1}L, \\ \tilde{\mu} &\geq (1 - \gamma\mu)^{K-1}\mu.\end{aligned}$$

Therefore, $\tilde{f}(x, \gamma, \Theta_{1:K})$ has condition number $\tilde{\kappa}$ satisfying

$$\tilde{\kappa} \leq \left(\frac{1 - \gamma L}{1 - \gamma\mu}\right)^{K-1} \frac{L}{\mu}.$$

Local computation as implicit regularization For $\Theta = \Theta_K$, we clearly see that as $K \rightarrow 1$ or $\gamma \rightarrow 0$, then $\tilde{\kappa} \rightarrow L/\mu$, the condition number of the true loss function. However, if γ is not close to 0, we see an exponential reduction (in terms of K) of the condition number. While the analysis is not quite as clear for $\Theta = \Theta_{1:K}$, one can show that for all γ , $\tilde{\kappa} \leq L/\mu$, with equality if and only if $\gamma = 0$ or $K = 1$. Moreover, the condition number decreases as $K \rightarrow \infty$ or $\gamma \rightarrow L^{-1}$.

It is well known that the condition number measures how quickly methods such as gradient descent can find a minimizer of a strongly convex function (see Chapter 3 of (Bubeck, 2017) for reference). By performing more local computations on the clients, and with larger learning rate, we actually reduce the condition number of the surrogate loss. We see that intuitive notions about methods such as FedAvg (e.g. that more local computation improves convergence) can be made formal by analyzing properties of the surrogate loss. Thus, we have the following important takeaway:

Methods such as MAML, FedAvg, and Reptile perform implicit regularization on the condition number of the surrogate loss function they are actually optimizing.

When $\Theta = \Theta_K$ or $\Theta_{1:K}$, we see that LOCALUPDATE may be able to optimize the surrogate loss more quickly (due to the condition number reduction). However, as shown in Section 4, the surrogate loss may differ drastically from the true loss. In the next section, we use the spectral properties of the surrogate loss derived above to quantify the distance between the minimizers of these two functions.

6. Bounding the distance between global minima

As discussed above, LOCALUPDATE is not optimizing the desired loss function $f(x)$, but a surrogate loss function $\tilde{f}(x, \gamma, \Theta)$. In this section, we will bound the distance between the minima of these two functions. We will assume that Assumptions 1, 2, and 3 hold throughout. Recall that by Lemma 13, as long as $\gamma < L^{-1}$, $\tilde{f}(x, \gamma, \Theta)$ is strongly convex and therefore has a unique minimizer.

For simplicity of notation, we will fix γ, Θ and let Q_i refer to $Q_i(\gamma, \Theta)$ throughout this section. We will also define matrices \tilde{A}_i and \tilde{A} , depending on Θ , as follows:

$$\tau := \left(\sum_{k=1}^{K(\Theta)} \theta_k \right)^{-1}, \quad \tilde{A}_i := \tau Q_i A_i, \quad \tilde{A} := \mathbb{E}_i [\tilde{A}_i]. \quad (19)$$

We also define the following quantities:

$$x^*(\gamma, \Theta) := \operatorname{argmin}_x \tilde{f}(x, \gamma, \Theta), \quad x^* := \operatorname{argmin}_x f(x).$$

By Lemma 5, if $\gamma = 0$ or $\theta_k = 0$ for $k \geq 2$, then $Q_i = \tau^{-1}I$. Therefore, $\tilde{f}(x, \gamma, \Theta) = \tau^{-1}f(x)$, and so $x^*(0, \Theta) = x^*$. However, for general γ and Θ , $x^*(\gamma, \Theta) \neq x^*$.

We are first interested in how far apart the two minimizers can possibly be. We first consider the asymptotic affect of K when setting $\Theta = \Theta_{1:K}$. In fact, varying K can only change the distance between the two by a fixed amount, as shown in the following.

Lemma 15 *Suppose $0 < \gamma < L^{-1}$. Then for all $K \geq 1$,*

$$\tilde{f}(x, \gamma, \Theta_{1:K}) \leq \frac{1}{2\gamma} \mathbb{E}_{i \sim \mathcal{P}} \|x - c_i\|^2.$$

Moreover, $\tilde{f}(x, \gamma, \Theta_{1:K})$ converges pointwise to this function, ie.

$$\lim_{K \rightarrow \infty} \tilde{f}(x, \gamma, \Theta_{1:K}) = \frac{1}{2\gamma} \mathbb{E}_{i \sim \mathcal{P}} [\|x - c_i\|^2]$$

which has a unique minimizer at $x = \mathbb{E}_{i \sim \mathcal{P}} [c_i] = c$.

Intuitively, we see that as long as the client learning rate is not too high, the worst possible surrogate loss is the one defined by the average distance to the client optimizers. Intuitively, as $K \rightarrow \infty$, LOCALUPDATE will take steps oriented more and more towards the average of the client minimizers (one-shot averaging), which is reflected in the experiment in Figure 1.

We now wish to understand the non-asymptotic regime, especially the distance between the surrogate risk minimizer and the true risk minimizer, as this will help inform us how to set γ in LOCALUPDATE. We have the following result.

Theorem 16 *If $\gamma < L^{-1}$, then*

$$\|x^*(\gamma, \Theta) - x^*\| \leq \frac{L\sigma_c}{\mu} \left(1 + \frac{\sigma_A}{\mu} \right) \frac{1 - \chi(\gamma, \Theta)}{\chi(\gamma, \Theta)} \quad (20)$$

where

$$\chi(\gamma, \Theta) := \frac{\sum_{k=1}^{K(\Theta)} \theta_k (1 - \gamma L)^{k-1}}{\sum_{k=1}^{K(\Theta)} \theta_k}. \quad (21)$$

When $\Theta = \Theta_{1:K}$ (as in FedAvg/Reptile), we can derive an even tighter bound that omits the direct dependency on L/μ . Recall that by Corollary 13, the condition number of $\tilde{f}(x, \gamma, \Theta_{1:K})$ is bounded above by

$$\tilde{\kappa} = \frac{\phi_{K,L}(\gamma)}{\phi_{K,\mu}(\gamma)}$$

where $\phi_{K,\lambda}(\gamma)$ is as in (17). We will see in the following theorem that the distance between minimizers is controlled by $\phi_{K,L}(\gamma)$ and $\phi_{K,\mu}(\gamma)$.

Theorem 17 *If $\gamma < L^{-1}$, then*

$$\|x^*(\gamma, \Theta_{1:K}) - x^*\| \leq \sigma_c \left(1 + \frac{\sigma_A}{\mu}\right) \frac{LK - \phi_{K,L}(\gamma)}{\phi_{K,\mu}(\gamma)}.$$

Informally, the term $LK - \phi_{K,L}(\gamma)$ measures the discrepancy between the surrogate loss function and the true loss function; as $\gamma \rightarrow 0$, $\phi_{K,L}(\gamma) \rightarrow LK$.

In order to get better control on Theorem 17 for $\gamma > 0$, we will show that when γ is sufficiently small, $\phi_{K,\lambda}(\gamma)$ is close to $K\lambda$.

Lemma 18 *Let $0 \leq \epsilon \leq 1 - e^{-K}$ and suppose*

$$\gamma \leq \frac{\ln(1/(1 - \epsilon))}{K\lambda}.$$

Then

$$\phi_{K,\lambda}(\gamma) \geq (1 - \epsilon)K\lambda.$$

This results in the immediate corollary.

Corollary 19 *Suppose $\epsilon \leq 1 - e^{-K}$ and*

$$\gamma \leq \frac{\ln(1/(1 - \epsilon))}{KL}.$$

Then

$$\phi_{K,L}(\gamma) \geq (1 - \epsilon)KL \quad \text{and} \quad \phi_{K,\mu}(\gamma) \geq (1 - \epsilon)K\mu.$$

Plugging these into Theorem 17, we get the following.

Corollary 20 *For $\epsilon \leq 1 - e^{-K}$, suppose*

$$\gamma \leq \frac{\ln(1/(1 - \epsilon))}{KL}.$$

Then

$$\|x^*(\gamma, \Theta_{1:K}) - x^*\| \leq \sigma_c \left(1 + \frac{\sigma_A}{\mu}\right) \frac{L}{\mu} \frac{\epsilon}{1 - \epsilon}.$$

We can also use a similar analysis to bound the distance between $x^*(\gamma, \Theta)$ for different values of γ . We will focus on the FedAvg/Reptile case. We will show that this distance depends on the discrepancy between the eigenvalues of the matrices $Q_i(\gamma, \Theta_{1:K})A_i$.

Theorem 21 *Let $\gamma_1 \leq \gamma_2 < L^{-1}$. Then*

$$\|x^*(\gamma_1, \Theta_{1:K}) - x^*(\gamma_2, \Theta_{1:K})\| \leq \sigma_c \left(1 + \frac{\phi_{K,L}(\gamma_2)}{\phi_{K,\mu}(\gamma_2)} \right) \left(\frac{\phi_{K,L}(\gamma_1) - \phi_{K,L}(\gamma_2)}{\phi_{K,\mu}(\gamma_1)} \right).$$

The presence of the ϕ terms makes the dependence on $|\gamma_1 - \gamma_2|$ somewhat opaque. In fact, we have the following simpler (though looser) bound.

Corollary 22 *Let $\gamma_1 \leq \gamma_2 < L^{-1}$. Then*

$$\|x^*(\gamma_1, \Theta_{1:K}) - x^*(\gamma_2, \Theta_{1:K})\| \leq 2\sigma_c \frac{L^3}{\mu^2} (\gamma_2 - \gamma_1).$$

One particularly useful consequence is that if the client learning rate satisfies $\gamma_t = c/t$ for some constant c , then

$$\|x^*(\gamma_{t+1}, \Theta_{1:K}) - x^*(\gamma_t, \Theta_{1:K})\| \leq O\left(\frac{1}{t^2}\right).$$

We will use this later to show that by decaying the client learning rate in this manner, successive model updates in LOCALUPDATE will be closely aligned.

7. Convergence of FedAvg/Reptile

We now wish to use Theorem 17 to understand how quickly FedAvg/Reptile with K local steps converges to x^* . However, by Lemma 3, we know that performing FedAvg/Reptile with a fixed client learning rate of γ will only result in convergence to $x^*(\gamma, \Theta_{1:K})$, the minima of the surrogate loss $\tilde{f}(x, \gamma, \Theta_{1:K})$, not to the true risk minimizer x^* . We will therefore analyze the convergence behavior of these algorithms with and without learning rate decay.

Our goal in this section is two-fold. First, we wish to understand the trade-offs incurred by performing local computation instead of mini-batch SGD. Second, we wish to show that by Theorem 3, we can analyze federated learning and meta-learning algorithms using classical optimization techniques. There are a large number of important works on federated optimization, that consider more general cases than ours. Unfortunately, the proof techniques behind many of these are relatively opaque, and require careful accounting of the bias incurred by performing local computation. This sometimes leads to either proof errors, or else omitted critical assumptions (Woodworth et al., 2020, Appendix A). Both of these can hinder understanding or make comparisons between convergence rates difficult. By contrast, while limited to a much narrower range of loss functions, our analysis uses essentially standard convex optimization analyses (such as by Rakhlin et al. (2012) and Bottou et al. (2018)), combined with the results from Section 6. We also emphasize that while we focus on FedAvg/Reptile, our results can be easily extended to more general instances of LOCALUPDATE.

7.1 Fixed client learning rate

We first wish to understand the setting where the client learning rate γ is fixed. Fix a client step-size γ and K , and for notational convenience, define

$$\begin{aligned}\tilde{f}_\gamma(x) &:= \tilde{f}(x, \gamma, \Theta_{1:K}), \\ \tilde{f}_\gamma^* &:= \min_x \tilde{f}_\gamma(x), \\ x_\gamma^* &:= \operatorname{argmin}_x \tilde{f}_\gamma(x).\end{aligned}$$

As γ tends towards 0, $\tilde{f}_\gamma(x)$ converges to the true loss function $f(x)$ (under different notions of convergence depending on the set of assumptions made). For example, under Assumption 2 this convergence will occur uniformly on \mathbb{R}^d .

Fix $\gamma_t = \gamma$ for all t in LOCALUPDATE. Then, at each iteration t the server starts at a point x_t which it broadcasts to some number of clients. The clients compute local updates q_t^i via InnerLoop(γ, Θ) (Algorithm 2), and send these values to the server. The server then computes the average q_t of the q_t^i and updates its model via $x_{t+1} = x_t - \eta_t q_t$.

Given a starting point x , we let $q_\gamma(x)$ denote the random vector computed by averaging M vectors of the form $q^i = \text{InnerLoop}(i, x, \gamma, \Theta)$ where $i \sim \mathcal{P}$. Thus, in Algorithm 1 with a constant client learning rate γ , $x_{t+1} = x_t - \eta_t q_\gamma(x_t)$. Recall that by Theorem 3,

$$\mathbb{E}[q_\gamma(x)] = \nabla \tilde{f}_\gamma(x).$$

Throughout this section, we will assume Assumptions 2 and 3, as well as the following ‘‘bounded variance’’ condition.

Assumption 4 For all x and i , $\mathbb{E}_{z \sim \mathcal{D}_i} \|\nabla_x f(x; z) - \nabla f_i(x)\|^2 \leq G^2$.

We can then translate this into a bound on the variance of $q(x, \gamma, \Theta_{1:K})$.

Lemma 23 Suppose Assumption 4 holds. Then for all $\gamma \geq 0$,

$$\mathbb{E} \|q_\gamma(x) - \nabla \tilde{f}_\gamma(x)\|^2 \leq \frac{KG^2}{MB}.$$

We will also use the following bound on the strong convexity parameter of our surrogate loss functions.

Lemma 24 Suppose that Assumption 2 holds. Then for all t , \tilde{f}_γ is μ_γ -strongly convex where

$$\mu_\gamma := \phi_{K, \mu}(\gamma) = \frac{1 - (1 - \gamma\mu)^K}{\gamma}.$$

and L_γ -smooth where

$$L_\gamma := \phi_{K, L}(\gamma) = \frac{1 - (1 - \gamma L)^K}{\gamma}.$$

Note that these results follow directly from Lemma 11 and the fact that the strong convexity and smoothness parameters are governed by the maximum and minimum eigenvalues of $Q_i(\gamma, \Theta_{1:K})A_i$.

Using techniques similar to those in (Rakhlin et al., 2012), we arrive at the following descent lemma.

Lemma 25 *Suppose that Assumptions 2 and 4 hold, and that we have step sizes $\{\eta_t\}_{t \geq 1}$ satisfying*

$$\eta_t \leq \frac{\mu_\gamma}{L_\gamma^2}. \quad (22)$$

Then

$$\mathbb{E}[\|x_{t+1} - x_\gamma^*\|^2] \leq (1 - \eta_t \mu_\gamma) \mathbb{E}[\|x_t - x_\gamma^*\|^2] + \eta_t^2 \frac{KG^2}{MB}.$$

On upper bounds for server learning rates Note that in Lemma 25, we assume a slightly stronger condition than is often assumed in optimization literature, namely that $\eta \leq 1/L_\gamma \kappa_\gamma$ where κ_γ is the condition number. Typically, works on optimization would only require η to be at most the inverse of the Lipschitz constant. While it is an open question as to whether this condition is necessary, there are a few relevant factors. First, we note that we can relax (22) to $\eta_t \leq L_\gamma^{-1}$ if we strengthen Assumption 4 to a bounded gradient assumption instead of a bounded variance assumption. Second, when γ is moderately large with respect to μ , Lemma 13 implies that $\mu_\gamma \approx L_\gamma$, so (22) gives a similar condition to assuming $\eta_t \leq L_\gamma^{-1}$. Finally, we note that a similar bound on the learning rate was used by Reisizadeh et al. (2020) in conjunction with a bounded variance assumption. While we conjecture that this condition can be relaxed, we leave this for future work.

Applying Lemma 25 repeatedly, we derive at the following.

Theorem 26 (Fixed client LR, fixed server LR) *Suppose that $\eta \leq \mu_\gamma/L_\gamma^2$. Then the outputs of LOCALUPDATE($\eta, \gamma, \Theta_{1:K}$) satisfy*

$$\mathbb{E}[\|x_{t+1} - x_\gamma^*\|^2] \leq (1 - \eta \mu_\gamma)^t \|x_1 - x_\gamma^*\|^2 + \frac{\eta KG^2}{\mu_\gamma MB}.$$

Many prior results for fixed client learning rate provide a bound of the same general form as Theorem 26 (ie. a sum of a decaying term and a constant error term), but bound the distance from x^* , rather than from x_γ^* . This makes the error term’s significance more opaque. While non-federated optimization results often have constant error terms due to stochasticity, in federated convergence results (eg. (Khaled et al., 2020, Theorem 5)), the constant term often does not disappear in deterministic setting ($G = 0$). To the reader, it may not be immediately clear why this is the case. This could be due to actual convergence properties, or due to the analysis not being tight. By contrast, our result shows that this error term is an inherent property of the algorithm, as in general, $x_\gamma^* \neq x^*$.

As is the case in general stochastic optimization, a constant learning rate is only sufficient to arrive in a neighborhood of the critical point of the underlying loss. However, this critical point is not the true risk minimizer x^* . As in Section 4, we see that in heterogeneous settings, client learning rate decay is necessary for convergence to the true risk minimizer.

To make the suboptimality gap tend towards zero, we must decay the server learning rate η over time, as in the following theorem.

Theorem 27 (Fixed client LR, decaying server LR) *Suppose that for all $t \geq 1$,*

$$\eta_t = \frac{a_\gamma}{b_\gamma + t} \text{ for } a_\gamma = \frac{2}{\mu_\gamma} \text{ and } b_\gamma \geq \frac{2L_\gamma^2}{\mu_\gamma^2}.$$

Then the outputs of LOCALUPDATE($\{\eta_t\}, \gamma, \Theta_{1:K}$) satisfy

$$\mathbb{E}[\|x_t - x_\gamma^*\|^2] \leq \frac{\nu_\gamma}{b_\gamma + t}$$

where

$$\nu_\gamma := \max \left\{ \frac{4KG^2}{\mu_\gamma^2 MB}, (b_\gamma + 1)\|x_1 - x_\gamma^*\|^2 \right\}.$$

We can now derive a convergence rate towards the true risk minimizer, x^* .

Corollary 28 *Fix ϵ satisfying $\epsilon \leq 1 - e^{-K}$. Suppose*

$$\gamma \leq \frac{\ln(1/(1 - \epsilon))}{KL}$$

and that η_t is as in Theorem 27. Then the outputs of LOCALUPDATE($\{\eta_t\}, \gamma, \Theta_{1:K}$) satisfy

$$\mathbb{E}[\|x_t - x^*\|^2] \leq \frac{2\nu_\gamma}{b_\gamma + t} + 2\sigma_c^2 \left(1 + \frac{\sigma_a}{\mu}\right)^2 \frac{L^2}{\mu^2} \frac{\epsilon^2}{(1 - \epsilon)^2}$$

where

$$\nu_\gamma \leq \max \left\{ \frac{4G^2}{(1 - \epsilon)^2 \mu^2 KMB}, (b_\gamma + 1)\|x_1 - x_\gamma^*\|^2 \right\}.$$

While notationally complex, this result has a few important facets. Define

$$\beta_1 = \frac{G^2}{(1 - \epsilon)^2 \mu^2 KMB}, \quad \beta_2 = (b_\gamma + 1)\|x_1 - x_\gamma^*\|, \quad \beta_3 = \sigma_c^2 \left(1 + \frac{\sigma_a}{\mu}\right)^2 \frac{L^2}{\mu^2} \frac{\epsilon^2}{(1 - \epsilon)^2}.$$

Thus, this result shows that,

$$\mathbb{E}[\|x_t - x^*\|^2] \leq \mathcal{O}\left(\frac{\max\{\beta_1, \beta_2\}}{t} + \beta_3\right).$$

As $\epsilon \rightarrow 0$, $\gamma \rightarrow 0$, LOCALUPDATE becomes roughly equivalent to mini-batch SGD with batches of size KB on M clients. In fact, β_1 is the convergence term we would derive from performing mini-batch SGD with batches of size KB on M clients per round. In particular, we get a variance reduction of $(KMB)^{-1}$. This variance reduction is similar in nature to work by Woodworth et al. (2020) in the homogeneous setting ($\sigma_A = \sigma_c = 0$), which shows an analogous improvement in convergence rates. Note that β_1 gets larger as ϵ gets larger. Thus, the variance reduction is reduced in heterogeneous settings.

The term β_2 measures the initial suboptimality to the surrogate loss function. It is here that having a small γ may incur a price. Note that b_γ is twice the condition number of \tilde{f}_γ . As shown in Corollary 13 and in the discussion thereafter, larger γ lead to smaller b_γ due to

the implicit regularization of local computation. Conversely, at $\gamma = 0$, $b_\gamma = 2L^2/\mu^2$, which may dominate β_1 . Thus, smaller γ lead to a larger effective initial suboptimality gap.

The last term β_3 measures the discrepancy between the surrogate loss function and the true loss function. If $\sigma_c = 0$, for instance, when the data is completely homogeneous, this discrepancy is 0. We then recover similar results to that of Woodworth et al. (2020), which shows a $1/K$ improvement in convergence for Local SGD with K steps, but in the heterogeneous setting. If $\sigma_c \neq 0$, we can still remove the effect of heterogeneity by setting $\epsilon = 0$ (which means setting $\gamma = 0$). In this case, FedAvg reduces to mini-batch SGD with batches of size KB on each client.

7.2 Decaying client and server learning rates

In this section, we will show that by decaying the client and server learning rates appropriately, we can derive a bound on $\|x_t - x^*\|^2$ that does not require setting the learning rates in terms of the desired optimality gap ϵ .

Throughout this section, we again focus on the FedAvg/Reptile setting. At every iteration t , we will use client learning rate γ_t and server learning rate η_t that decay at a $1/t$ rate. Let $\kappa = L/\mu$ denote the condition number of $f(x)$. We have the following theorem.

Theorem 29 (Decaying client LR, decaying server LR) *Let*

$$\eta_t = \frac{a_t}{b+t} \quad \text{for } a_t = \frac{3}{\mu_t} \quad \text{and } b = 3\kappa^2$$

and let

$$\gamma_t = \min \left\{ \frac{1}{L(b+t)}, \frac{\ln(2)}{K\mu} \right\}.$$

Suppose we run LOCALUPDATE with γ_t, η_t as above and $\Theta = \Theta_{1:K}$ to produce iterates x_t . Then for all $t \geq 1$,

$$\mathbb{E}[\|x_t - x^*\|^2] \leq \frac{2\nu + 16\sigma_c^2\kappa^2}{b+t}.$$

where

$$\nu := \max \left\{ \frac{18G^2}{\mu^2 KMB}, (b+1)\|x_1 - x_1^*\|^2 \right\}.$$

No attempt was made to optimize constants. Rather, the point was to show that we can derive bounds on the distance to the true risk minimizer x^* that hold for all t and that help illustrate the implicit trade-offs in LOCALUPDATE. In particular, we do not require that γ , η , or t be defined in terms of the desired suboptimality gap ϵ . Rather, all that was required was learning rate decay on the order of $O(1/t)$ at both the server and the client.

Recall that by Theorem 26, some form of learning rate decay is necessary for convergence to the true risk minimizer. We therefore see that in some settings, learning rate decay is sufficient for LOCALUPDATE to converge to the true risk minimizer. While this was previously shown in the finite-sum setting for strongly convex functions by Li et al. (2020c), this result required bounded gradients, and did not illustrate the trade-offs in using FedAvg/Reptile over mini-batch SGD.

Comparison to mini-batch SGD Similar to Theorem 1 of (Woodworth et al., 2020), we see that performing LOCALUPDATE incurs a kind of variance reduction of $1/MB$ when compared to performing vanilla SGD over a shuffled version of the entire dataset. We also see that using LOCALUPDATE with $\gamma > 0$ does incur a potential benefit: Rather than having the convergence depend on the suboptimality gap $\|x_1 - x^*\|^2$ (as is the case for mini-batch SGD), it depends on $\|x_1 - x_1^*\|^2$. This may be much smaller depending on the initialization. For example, recall that by Lemma 15, if $\gamma_1 > 0$, then as $K \rightarrow \infty$, x_1^* tends to the “one-shot average” of the client minimizers, which typically requires many fewer communication rounds to estimate than the true risk minimizer. However, this reduction only benefits the convergence up to a point, in which case it becomes beneficial to use smaller γ .

As suggested by lower bounds on FedAvg in (Karimireddy et al., 2019) on FedAvg, our bounds do not show that FedAvg always converges faster than mini-batch SGD, and in fact, doing so may not be possible without further assumptions (such as a bound on the heterogeneity among clients) or more sophisticated optimization techniques (such as the use of control variates in SCAFFOLD (Karimireddy et al., 2019)).

While our theoretical results are only valid for the case of quadratic loss functions, we conjecture that even in much broader settings, the choice of learning rate γ still dictates a trade-off between accuracy and initial convergence. we will show in the next section that this holds empirically, even in non-convex settings.

8. Experimental results

In this section, we analyze LOCALUPDATE empirically, in order to understand how the choice of client and server learning rates impact convergence in more realistic machine learning tasks. In particular, we focus on (not necessarily convex) tasks and datasets that reflect federated learning in practice. We will show that both the choice of client learning rate and tuning of the corresponding server learning rate can be vital to attain the best performance of LOCALUPDATE, especially in limited communication settings.

Datasets and models We use four different datasets: the federated extended MNIST dataset (FEMNIST) (Caldas et al., 2018), the federated version of CIFAR-100 created by Reddi et al. (2020), the Shakespeare dataset (Caldas et al., 2018) and the Stack Overflow dataset (Authors, 2019). The first two are image datasets, the second two are text datasets. All datasets are publicly available. We specifically use the versions available in TensorFlow Federated (Ingerman and Ostrowski, 2019). All four datasets contain training and test clients. For the purposes of our experiments, we only use the training clients, as our work only concerns the loss of clients in the training population. Notably, our work does not broach the subject of generalization, which we leave to future work. The number of clients and examples in each dataset is presented in Table 1.

For FEMNIST, we train a moderately-sized CNN (the same as used in (McMahan et al., 2017)) to perform character recognition. For CIFAR-100, we train a ResNet-18 (where we replace the batch norm layers with group norm, as suggested by (Hsieh et al., 2019) and used by (Reddi et al., 2020)). For Shakespeare, we train an RNN with 2 LSTM layers to perform next-character-prediction. For Stack Overflow, we perform two distinct task: tag prediction (TP) and next-word-prediction (NWP). For Stack Overflow TP, we use a logistic regression classifier with one-versus-all classification. Note that this implies that Stack Overflow TP is

Table 1: Dataset statistics.

| DATASET | # OF CLIENTS | TOTAL # OF EXAMPLES |
|----------------|--------------|---------------------|
| CIFAR-100 | 500 | 50,000 |
| FEMNIST | 3,400 | 671,585 |
| SHAKESPEARE | 715 | 16,068 |
| STACK OVERFLOW | 342,477 | 135,818,730 |

a *convex* task. For Stack Overflow NWP, we train an RNN with 1 LSTM layer to perform next-word-prediction. These five tasks were previously analyzed by Reddi et al. (2020) for the purposes of comparing adaptive and non-adaptive federated optimization methods. For further details on datasets and models, see Appendix C.

Implementation and hyperparameters We implement LOCALUPDATE in TensorFlow Federated (Ingerman and Ostrowski, 2019). In all experiments, the set of clients \mathcal{I} is finite and we let \mathcal{P} be the uniform distribution over these clients. Each \mathcal{D}_i is the uniform distribution over some finite set of client examples. We analyze the performance of LOCALUPDATE with $\Theta = \Theta_{1:10}$ (ie. FedAvg/Reptile with $K = 10$ local steps) across the tasks discussed above. For FEMNIST, CIFAR-100, and Shakespeare, we sample $M = 10$ clients per round, while for Stack Overflow, we sample $M = 50$ clients (due to its much larger number of clients). In order to derive fair comparisons for different hyperparameter settings, we use a random seed to determine which clients are sampled at each round from \mathcal{P} . All plots are made using the same seed. We sample clients without replacement within each round, but with replacement across rounds. We use a batch size of $B = 20$ for FEMNIST and CIFAR-100, $B = 4$ for Shakespeare, and $B = 16$ for Stack Overflow.

8.1 Fixed server learning rates

We first perform a comparable analysis to that in Section 4 above for FEMNIST, CIFAR-100, and Shakespeare. Namely, we fix the server learning rate $\eta = 0.01$, and see how the training loss varies as a function of the client learning rate γ . We vary γ over

$$\gamma \in \{0, 10^{-3}, \dots, 10^{-1}, 1, 10, 10^2\}$$

and omit results that diverged due to the client learning rate being set too large. We plot the true loss function $f(x)$ (defined in (2)) in Figure 2.

We see that on all three tasks, especially CIFAR-100, the choice of client learning rate can impact not just the speed of convergence, but what point the algorithm converges to. In general, we see very similar behavior to that in Section 4, despite the non-convex loss functions involved in all three tasks. For both FEMNIST and CIFAR-100, smaller client learning rates eventually reach lower training losses than higher learning rates. This is particularly evident in the results for CIFAR-100. While $\gamma = 10^{-2}$ initially performs better than all other methods, it is eventually surpassed by $\gamma = 10^{-3}$, and $\gamma = 0$ ends up obtaining a comparable accuracy. Conversely, setting $\gamma = 1.0$ results in a sub-optimal training loss.

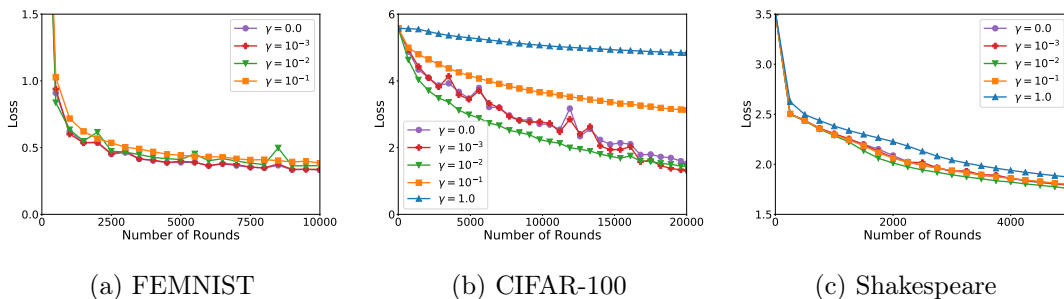


Figure 2: Cross-entropy training loss of LOCALUPDATE with fixed server learning rate $\eta = 0.01$ and $\Theta = \Theta_{1:10}$, and varying client learning rate γ .

We also see that while suboptimality gaps exist for FEMNIST and Shakespeare, they are much smaller than for CIFAR-100. Thus, our results also suggest that the theoretical suboptimality of larger γ may not be as important a facet in practice. We see here that despite the asymptotic suboptimality of FedAvg with $\gamma > 0$, in realistic settings where the number of communication rounds is limited, there may be little to no disadvantage to using $\gamma > 0$. In fact, as we see for CIFAR-100, there may be advantages to using larger γ in settings with relatively few communication rounds.

8.2 Deriving fair comparisons between different client learning rates

While the results in the previous section indicate the importance of γ , these comparisons are in some sense unfair. In particular, there is no reason that we need to fix the server learning rate η across different values of γ . In fact, this ignores differences in the Lipschitz constant of the associated surrogate loss functions. As shown in Corollary 13, choosing smaller γ increases the Lipschitz constant L_γ of the surrogate loss function, which in turn generally necessitates a smaller server learning rate. Thus, choosing larger γ enable higher values of η . To justify this further, we plot the ℓ_2 norm of the update applied to the server model at each round. That is, recall that in Algorithm 1, we update the model via

$$x_{t+1} = x_t - \eta q_t.$$

In Figure 3, we plot $\|q_t\|$ for different choices of γ in the CIFAR-100 task. Specifically, we plot the mean value of $\|q_t\|$ for each consecutive 1000 rounds, as well as the standard deviation within those rounds.

As expected, the ℓ_2 norm of the updates is highly dependent on the choice of γ . In particular, smaller learning rates lead to larger model updates. We also see that the absolute variance of the model update norm increases as well. As discussed after Corollary 28, the variance reduction offered by setting γ small SGD is potentially at odds with the increase in the condition number increase, a phenomenon reflected in Figure 3. Thus, we see that to derive a fair comparison between client learning rates, we must also allow the server learning rate to increase as the client learning rate increases.

One important caveat to this observation is that it is not enough to simply directly tie the client and server learning rate together. This is in fact what is done in the original incarnation of FedAvg in (McMahan et al., 2017). As discussed in Section 2.1, the original

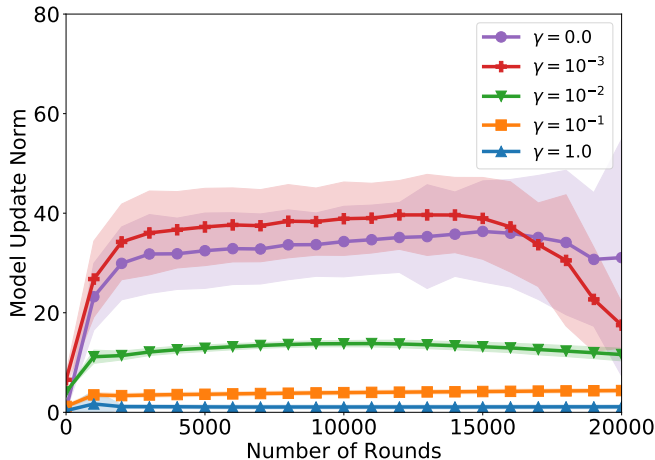


Figure 3: The ℓ_2 norm of the model update of LOCALUPDATE on CIFAR-100 at each round with fixed server learning rate $\eta = 0.01$ and varying client learning rate γ . We plot the mean ℓ_2 norm across every consecutive 1000 rounds (bold lines), as well as the standard deviation across these rounds (pale regions).

“vanilla” FedAvg algorithm corresponds to LOCALUPDATE with $\Theta = \Theta_{1:K}$ and $\gamma = \eta$. This does allow for the use of larger server learning rates with smaller client learning rates. However, this is not enough to necessarily derive optimal performance of LOCALUPDATE.

To demonstrate this, we plot the performance of LOCALUPDATE with $\eta = \gamma$ and $\Theta = \Theta_{1:10}$ for the CIFAR-100 task in Figure 4. We see results in stark contrast to Figure 2(b). In particular, $\gamma = 1.0$ actually results in an increased training loss, and $\gamma = 0.1$ outperforms $\gamma = 0.01$ for most rounds. Moreover, by setting $\gamma = \eta$, we do not allow $\gamma = 0$, even though $\gamma > 0$ necessarily results in a surrogate loss that does not match the true training loss. While this version of FedAvg is convenient from an implementation and hyperparameter tuning point of view, it does not result in the best performance of LOCALUPDATE. As we show in the next section, we can greatly improve performance by tuning client and server learning rates separately.

8.3 On the importance of tuned server learning rates

Based on the discussion in the section above, to give the most fair comparisons between different values of γ in LOCALUPDATE, we must also tune the server learning rate η . We perform the same experiments as in Figure 2, but where we tune the server learning rate η for each choice of γ . We vary η over

$$\eta \in \{10^{-3}, 10^{-2.5}, \dots, 10^1\} \quad (23)$$

and select η that results in the smallest average training loss over the last 100 rounds. We note that we use this averaging method as a single round of federated learning only samples a small number of clients. We plot the loss of LOCALUPDATE under these settings in Figures 5. For a list of all client learning rates and the corresponding best server learning rate for each task, see Appendix D.

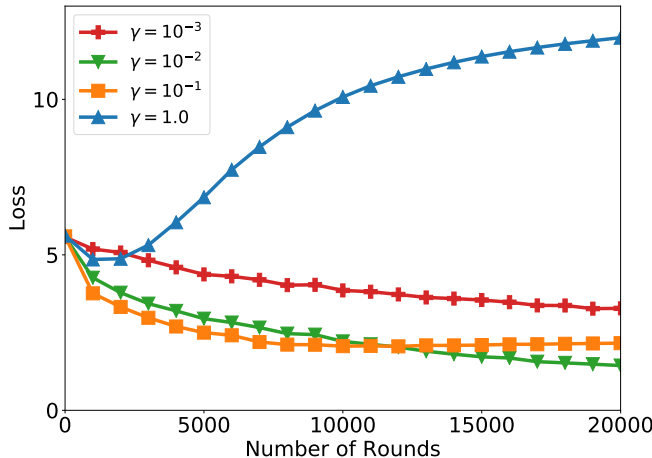


Figure 4: Cross-entropy training loss of LOCALUPDATE with $\Theta = \Theta_{1:10}$ and $\gamma = \eta$ for varying values of γ on the CIFAR-100 task.

Notably, we still see the same general trend discussed in our convergence rates in Section 7. While large values of γ may obtain a smaller training loss initially, eventually smaller values of γ perform comparably, if not better. However, it is instructive to note that this may take many thousands of communication rounds. In particular, for all three tasks, we see that $\gamma = 0$ does not perform comparably larger γ until near the end of our training procedure. We thus see the following:

By performing appropriate server and client learning rate tuning, we can mitigate the suboptimality of FedAvg/Reptile for $\gamma > 0$, especially when the number of communication rounds is limited.

In particular, our empirical results suggest that in realistic federated learning training tasks, the suboptimality of FedAvg/Reptile may only be an asymptotic concern. If we can only perform a limited number of training rounds, it often does benefit us to use larger values of γ . We note that this aligns with our discussion of how $\gamma > 0$ leads to condition number regularization (see Corollary 13).

8.4 Adaptive optimization and LOCALUPDATE

In order to understand the behavior of LOCALUPDATE more generally, we perform similar experiments on the Stack Overflow dataset. However, as shown by Reddi et al. (2020), performance of FedAvg on next-word-prediction tasks can be greatly improved by the use of adaptive optimization. In particular, Reddi et al. (2020) found that the use of the YOGI optimizer (Zaheer et al., 2018) improved performance in a wide variety of settings, including on the same tag-prediction and next-word-prediction tasks. Note that the YOGI optimizer is similar to the ADAM optimizer (Kingma and Ba, 2014), except that it uses a kind of *additive* adaptive update that can improve convergence by making more controlled progress. For more details, see (Zaheer et al., 2018).

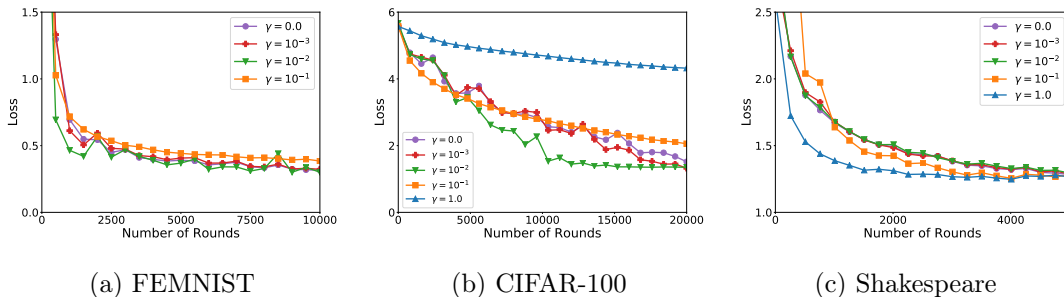


Figure 5: Cross-entropy training loss of LOCALUPDATE with $\Theta = \Theta_{1:10}$, varying client learning rate γ , and tuned server learning rate η .

Thus, for these tasks, we use a modified version of LOCALUPDATE in which the server uses the client update q_t as an estimate of the gradient of the loss function, and applies YOGI to this gradient. That is, we use Algorithm 1, but update the model via

$$x_{t+1} = \text{YOGI}(x_t, q_t, \eta_t).$$

We use the version of YOGI proposed by Zaheer et al. (2018), with first momentum term of $\beta_1 = 0.9$, second momentum parameter of $\beta_2 = 0.99$, an initial accumulator value of 0, and an ϵ value of 10^{-5} . We then perform analogous experiments to those above, where we first fix $\eta = 0.01$ and vary γ . However, due to the size of the Stack Overflow dataset (see Table 1), we did not compute the total loss $f(x)$ over all clients. Instead, we plot the average loss of the clients that participated in a given round, *before* local training occurs. This “loss at current round” can be viewed as a stochastic estimate of the true loss $f(x)$. This loss is plotted in Figure 6. We also perform experiments where we vary γ and tune η . We select the value of η with the smallest average training loss over the last 100 communication rounds. The result is given in Figure 7. For a list of all client learning rates and the corresponding best server learning rate for each task, see Appendix D.

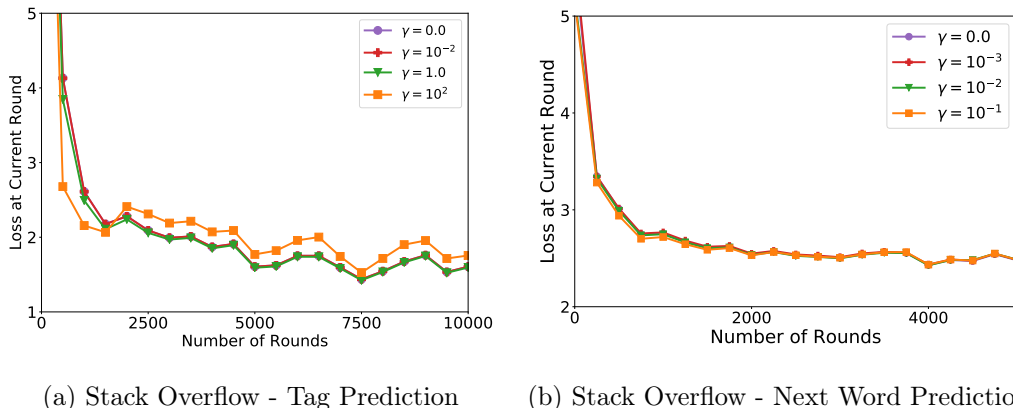


Figure 6: Cross-entropy training loss of LOCALUPDATE with server YOGI and $\Theta = \Theta_{1:10}$ on Stack Overflow with varying client learning rate γ and fixed server learning rate $\eta = 0.01$.

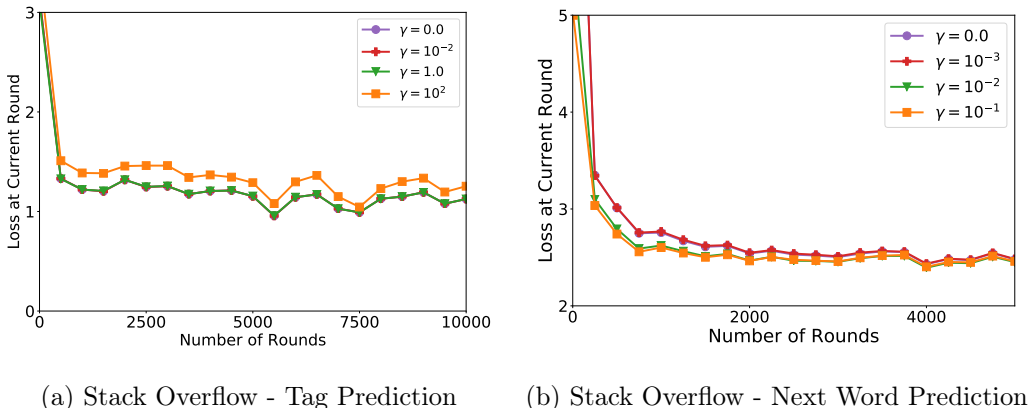


Figure 7: Cross-entropy training loss of LOCALUPDATE with server YOGI and $\Theta = \Theta_{1:10}$ on Stack Overflow with varying client learning rate γ and tuned server learning rate η .

For fixed η , large γ leads to an initially smaller loss that is eventually beaten or matched by smaller γ . However, we see similar behavior among all but the largest γ in both tasks, potentially due to the adaptivity in YOGI. Looking at Figure 7, we see that tuning the server learning rate has slightly different effects on the two tasks: While Stack Overflow TP with tuned η leads to the smaller γ performing better throughout the training process, Stack Overflow NWP with tuned η actually allows larger γ to achieve lower loss throughout. Notably, we see that the gap between large γ and small γ in Stack Overflow NWP winnows as the number of rounds increases. Our results reinforce the notion that in communication-limited settings, server learning rate tuning is critical to ensure the best performance possible. This holds even when not using SGD on the server, but instead using an adaptive optimizer.

9. Automatic learning rate decay

In short, our results in the section above suggest that depending on the desired number of communication rounds, we may wish to use different client learning rates. Unfortunately, this requires a large degree of hyperparameter tuning. Both the client and server learning rate must be tuned. However, if the number of communication rounds in a federated learning system is limited, it may not be feasible to conduct extensive hyperparameter tuning, as the communication rounds required to do so may be better utilized by training your model for more rounds.

To help reduce the amount of learning rate tuning required, we propose a method for automatic learning rate decay that helps mitigate the need for *client* learning rate tuning. Our method will utilize our theoretical and empirical observations above showing that large client learning rates should be used initially, while smaller learning rates eventually reach a lower training loss. By decaying the client learning rate automatically over time, we mitigate the need to tune it. Instead, it can be set to any moderate value that does not result in divergent behavior on clients. We will be particularly concerned with systems-level constraints (such as those encountered in federated learning) when describing our method.

One particularly important restriction in many local update settings is the ability to compute the training loss $f(x)$. Recall that we defined

$$f(x) := \mathbb{E}_{i \sim \mathcal{P}} [f_i(x)], \quad f_i(x) := \mathbb{E}_{z \sim \mathcal{D}_i} [f(x; z)]$$

where \mathcal{P} is a distribution over clients, and \mathcal{D}_i is the client’s data distribution. In settings with limited communication, it may not be feasible to sample most or even a moderate fraction of the clients from \mathcal{P} . Moreover, sampling a client $i \sim \mathcal{P}$ purely for the purposes of estimating the loss may be a waste of resources, as that client could be used for training purposes.

Thus, we propose a version of LOCALUPDATE that simultaneously computes local updates and estimates the loss function. Specifically, at each round t , we sample a set I_t of clients of size M . For each $i \in I_t$, we first compute an estimate ℓ_t^i of the local loss function $f_i(x_t)$, as well as the client’s model update q_t^i as defined in Algorithm 2. Note that it is important that $f_i(x_t)$ is estimated *before* computing any local updates, as otherwise we risk overfitting to the client’s dataset. The server then computes

$$\ell_t := \frac{1}{M} \sum_{i \in I_t} \ell_t^i, \quad q_t := \frac{1}{M} \sum_{i \in I_t} q_t^i. \quad (24)$$

As in LOCALUPDATE, we will use this q_t to update the model. The loss estimate ℓ_t will be used to determine whether to decay the client or server learning rates. We will use the strategy of decaying learning rates on plateaus. If the loss f_t is not sufficiently small, we will decay the client and server learning rates. We record the minimum loss seen up to round t , and then check if

$$\ell_t < \min_{j < t} \ell_j - \Delta$$

for some small $\Delta > 0$. Intuitively, if the loss ℓ_t has not decreased sufficiently, we may be at a suboptimal point (due to a large client learning rate γ) and therefore should decrease γ , which necessitates a decrease in η . We propose decaying γ and η by fixed factors $\alpha, \beta \in (0, 1)$, as this kind of “staircase” learning rate schedule has been repeatedly demonstrated to perform well across many tasks (Krizhevsky, 2014; Goyal et al., 2017). A full version of this algorithm, which we refer to as LOCALUPDATEDECAY, is given in Algorithms 3 and 4.

9.1 Practical refinements to LOCALUPDATEDECAY

In this section we describe three practical refinements to LOCALUPDATEDECAY that can improve convergence behavior. First, in settings where the number of clients sampled per round M is sufficiently small compared to $|\mathcal{I}|$, we can instead estimate the loss by using a moving window average across rounds. That is, given some window size $W > 0$, we can compute an estimate of the loss $\hat{\ell}_t$ with reduced variance via

$$\hat{\ell}_t = \frac{1}{W} \sum_{j=0}^{W-1} \ell_{t-j}$$

where f_t is as in (24). This is the average loss of all clients in the last W rounds. Note that Algorithm 3 corresponds to $W = 1$. We would then decay the client and server learning

Algorithm 3 LOCALUPDATEDECAY:

Outer Loop

OuterLoop($x, \eta, \gamma, \Theta, \Delta > 0, \alpha, \beta \in (0, 1)$): $x_1 = x$ **for** each round $t = 1, 2, \dots, T$ **do** $I_t \leftarrow$ (random set of M clients)**for** each client $i \in I_t$ **in parallel do** $\ell_t^i, q_t^i \leftarrow$ InnerLoop(i, x_t, γ, Θ) $\ell_t \leftarrow (1/M) \sum_{i \in I_t} \ell_t^i$ $q_t \leftarrow (1/M) \sum_{i \in I_t} q_t^i$ $x_{t+1} = x_t - \eta_t q_t$ **if** $\ell_t > \min_{j < t} \ell_j - \Delta$ **then** $\gamma \leftarrow \alpha\gamma, \eta \leftarrow \beta\eta$ **return** x_{T+1} **Algorithm 4** LOCALUPDATEDECAY:

Inner loop

InnerLoop(i, x, γ, Θ): $x_1 = x$ $\ell \leftarrow \mathbb{E}_{z \sim \mathcal{D}_i} [f(x; z)]$ **for** $k = 1, 2, \dots, K(\Theta)$ **do**sample a set S_k of size B from \mathcal{D}_i $g_k = (1/B) \sum_{z \in S_k} \nabla f(x_k; z)$ $x_{k+1} \leftarrow x_k - \gamma g_k$ **return** $\ell, \sum_{k=1}^{K(\Theta)} \theta_k g_k$

rates if

$$\hat{\ell}_t > \min_{j < t} \hat{\ell}_j - \Delta. \quad (25)$$

Second, even using moving windows to estimate $f(x)$, the heterogeneity of clients can still cause problematic variance. Thus, one can instead decay the learning rates if there has been no progress (relative to Δ) for P consecutive rounds. That is, we keep a counter for how many consecutive rounds the condition (25) holds. If this counter ever reaches P , we then decay γ and η . If

$$\hat{\ell}_t \leq \min_{j < t} \hat{\ell}_j - \Delta$$

then we reset the counter to 0. Note that Algorithm 3 corresponds to $P = 1$.

Last, it is often useful to have a *cooldown period* C , where after decaying the learning rates γ and η , we do not decay the learning rate for the next C rounds. This is beneficial both for recovering a new estimate of the loss function, and for ensuring that the learning rate does not decay too frequently. Additionally, we recommend using this cooldown period for the first C rounds as well, as this allows one to develop a better estimate of $f(x)$ before decaying the learning rate.

While in practice, setting W, P , and C may seem difficult, we found that setting them all to be the same value led to good behavior across datasets and tasks. Moreover, the value can be estimated using simple heuristics. For example, suppose that we think that N randomly sampled clients are sufficient to give a good representation of \mathcal{P} . Then, $P = W = C = \lceil N/M \rceil$ should serve as a default value for these parameters. In practice, we found that fixing all three values to some moderate constant (ex. $P = W = C = 100$) was sufficient, even across datasets with widely varying numbers of clients.

9.2 Empirical evaluation

The primary motivation for LOCALUPDATEDECAY is removing the need for client learning rate tuning. Intuitively, we can use any moderately large value of γ that results in non-

divergent client behavior, and this will be gradually scaled back over time as we reach sub-optimal critical points of the corresponding surrogate loss. To validate this, we compare LOCALUPDATEDECAY to LOCALUPDATE on FEMNIST, CIFAR-100, Shakespeare, and Stack Overflow. For Stack Overflow, we again use a modified version where we apply YOGI on the server. In particular, we compare tuned but constant γ and η , to LOCALUPDATEDECAY.

Implementation and hyperparameters We implement LOCALUPDATEDECAY in TensorFlow Federated as well. When computing the client’s loss estimate ℓ , we compute the average loss over the entire client dataset. Unlike in the previous section, we do not tune the client learning rate γ . We instead vary γ over $\{10^2, 10, 1, 10^{-1}, 10^{-2}\}$ and select the largest γ that results in a non-divergent training loss, as we intend to test the hypothesis that LOCALUPDATEDECAY does not need γ to be tuned in the same way that LOCALUPDATE does. In all settings, we still tune the server learning rate, as this is can be vital for getting accurate and fair comparisons (as discussed in Section 8.3). We use the same server learning rate grid as with LOCALUPDATE, given in (23), and select the value that reaches the lowest average training loss over the last 100 communication rounds. A table of learning rates used by LOCALUPDATEDECAY for each task is given in Table 2.

Table 2: Client learning rate γ and server learning rate η used in LOCALUPDATEDECAY, in base-10 logarithm format.

| TASK | γ | η |
|-------------------|----------|--------|
| CIFAR-100 | 0 | -1 |
| FEMNIST | -1 | -1 |
| SHAKESPEARE | 0 | 3/2 |
| STACKOVERFLOW NWP | -1 | -3/2 |
| STACKOVERFLOW TP | 2 | 0 |

We tune no other hyperparameters. In LOCALUPDATEDECAY, specifically Algorithm 3, we set $\Delta = 10^{-4}$, $\alpha = 0.1$, $\beta = 0.9$. We also use the practical refinements discussed in Section 9.1, setting $P = W = C = 100$. All other parameters are identical to that of standard LOCALUPDATE.

Results For FEMNIST, CIFAR-100, and Shakespeare, we plot the results in Figure 8, where we also compare to the tuned results in Section 8.3. We find that in all three tasks, LOCALUPDATEDECAY eventually does as well as LOCALUPDATE with tuned γ , without the need for client learning rate tuning. For FEMNIST and Shakespeare, we find that LOCALUPDATEDECAY almost immediately does better than LOCALUPDATE and continues to do at least as well throughout the course of training, often better. While this is not true for CIFAR-100, the results are still instructive. We see that while the client learning rate is initially set to a suboptimal value ($\gamma = 1.0$), the automatic learning rate decay enables us to move away from this suboptimal basin and towards something comparable to the best tuned client learning rate after enough rounds. We see that despite initializing with a bad γ , the

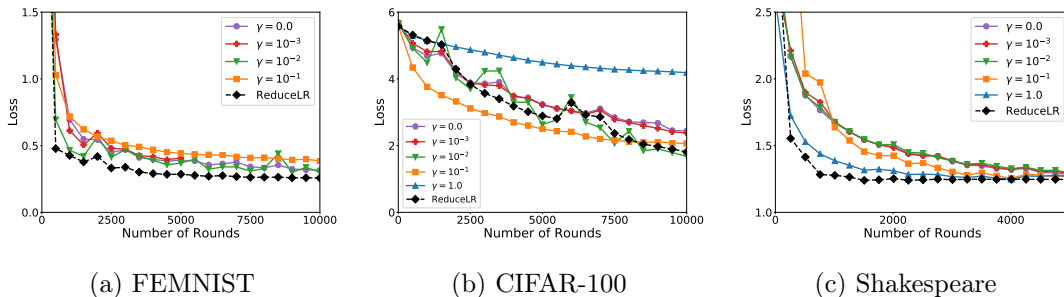


Figure 8: Cross-entropy training loss of LOCALUPDATE with $\Theta = \Theta_{1:10}$, varying client learning rate γ , and tuned server learning rate η . We also plot the cross-entropy loss of LOCALUPDATEDECAY with tuned server learning rate (ReduceLR).

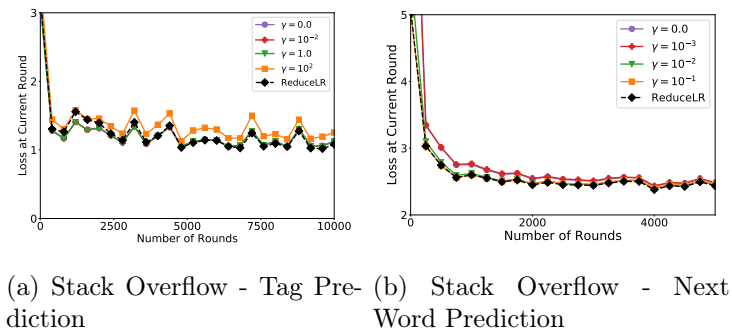


Figure 9: Cross-entropy training loss of LOCALUPDATE with server YOGI and $\Theta = \Theta_{1:10}$. We vary the client learning rate γ and tune the server learning rate η . We also plot the cross-entropy loss of LOCALUPDATEDECAY with server YOGI and tuned server learning rate (ReduceLR).

non-divergence in earlier rounds is sufficient to allow eventually near-optimal performance in the later rounds.

For both Stack Overflow tasks we plot an analogous results in Figure 9. As discussed in Section 8.4, due to the size of the Stack Overflow dataset, we do not plot the loss $f(x)$ over all clients. Instead, we plot the average loss among all clients in each round before training. For Stack Overflow NWP, we see that LOCALUPDATEDECAY performs comparably to the best tuned client learning rate. However, for Stack Overflow TP, we see that the decay actually helps significantly. While we initialize with a suboptimal client learning rate $\gamma = 100$, (which clearly achieves higher loss throughout), by decaying the client learning rate we are able to obtain comparable or lower loss than all other fixed γ .

10. Open questions

Our work above opens up a number of possible follow-up directions in the area of federated optimization. First, we expect the same kind of analysis obtained above to apply to methods similar to LOCALUPDATE. For example, while the FedProx algorithm (Li et al., 2019) does

not fit the format of LOCALUPDATE as presented in this work, we believe that it can be analyzed in a similar way. As shown by Pathak and Wainwright (2020), even in the non-stochastic setting, FedProx is not optimizing the true loss function. Thus, a natural question is to understand exactly what loss function is being optimized, and how the structure of FedProx encourages convergence over FedAvg. Another natural algorithm for analysis is a more general version of LOCALUPDATE in which the client learning rate is decayed during a client’s local computation. This may help combat adverse effects incurred by setting K to be too large.

More generally, we would also like to understand the behavior of LOCALUPDATE on non-quadratic functions. Even generalizing the analysis above to the strongly convex case would be substantial progress towards understanding federated learning in heterogeneous settings. While there may be no surrogate loss that LOCALUPDATE is directly optimizing through SGD, we believe that the intuition behind our work can still be carried forward for more general loss functions. In particular, one might expect that the optimization dynamics of LOCALUPDATE can be parameterized in terms of γ and Θ , even in non-quadratic settings, and that the selection of these parameters governs a trade-off between the speed of convergence and the accuracy of the resulting critical point.

Another interesting open direction is determining how to best set Θ for a given problem. As seen above, the choice of Θ drastically alters optimization dynamics. While it is often chosen in an ad hoc manner (based in part on the cost of communication), one could imagine attempting to minimize the number of rounds need to obtain a given accuracy level with respect to Θ . Even for FedAvg/Reptile, it is not clear how to set the number of local steps K . Insights into this could greatly improve the performance of federated learning algorithms.

Finally, we note that our work is fundamentally concerned with the training dynamics of local update methods. In practice, we are often instead interested in the generalization ability of a model. We suspect that the choice of parameters in LOCALUPDATE can have large implications for generalization ability, the study of which we leave to future work.

Acknowledgments

We would like to thank Keith Rush and Sai Praneeth Karimireddy for the remarks that accidentally helped spark this work. We would also like to thank H. Brendan McMahan and Zachary Garrett for fruitful discussions about decoupling client and server learning rates in federated learning. Finally, we gratefully acknowledge Shanshan Wu for insights on personalization in federated learning.

Appendix A. Relation between FedAvg, Local SGD, and LOCALUPDATE

In this section, we formalize the connection between FedAvg, Local SGD, and LOCALUPDATE. First, we note that in common descriptions of FedAvg and Local SGD algorithms (see (McMahan et al., 2017) and (Stich, 2019) for example), these two are effectively the same algorithm. The difference in nomenclature often reflects the distributed setting: Local SGD is often referred to in settings with homogeneous data, while FedAvg is often used in heterogeneous settings, especially for the purposes of federated learning.

We will use the following (simplified) version of the algorithms: At each iteration t of FedAvg/Local SGD, we have some set of clients I_t of size M . Each client $i \in I_t$ receives the server’s model x_t , and applies K steps of mini-batch SGD updates to its local model to create an updated local model x_t^i . The server then updates its model via

$$x_{t+1} = \frac{1}{M} \sum_{i \in I_t} x_t^i.$$

Fix t , and let g_k^i denote the k -th mini-batch gradient of client i . Suppose we use a learning rate of γ on each client when performing mini-batch SGD. Then we have

$$\begin{aligned} x_{t+1} &= \frac{1}{M} \sum_{i \in I_t} x_t^i \\ &= x_t - \frac{1}{M} \sum_{i \in I_t} (x_t - x_t^i) \\ &= x_t - \frac{1}{M} \sum_{i \in I_t} x_t - \left(x_t - \gamma \sum_{k=1}^K g_k^i \right) \\ &= x_t - \gamma \frac{1}{M} \sum_{i \in I_t} \sum_{k=1}^K g_k^i. \end{aligned}$$

This is exactly LOCALUPDATE with $\Theta = \Theta_{1:K}$ and $\eta = \gamma$. However, by allowing η to vary independently of γ in LOCALUPDATE, we can obtain markedly different convergence behavior. We note that a form of this decoupling has previously been explored by Karimireddy et al. (2019) and Reddi et al. (2020). However, these versions instead perform averaging on the so-called “model delta” (see (Reddi et al., 2020)), in which the server model is updated via

$$\begin{aligned} x_{t+1} &= x_t - \frac{\eta}{M} \sum_{i \in I_t} (x_t - x_t^i) \\ &= x_t - \frac{\eta}{M} \sum_{i \in I_t} \left(x_t - \left(x_t - \gamma \sum_{k=1}^K g_k^i \right) \right) \\ &= x_t - \frac{\eta\gamma}{M} \sum_{i \in I_t} \sum_{k=1}^K g_k^i. \end{aligned}$$

Thus, while this does decouple η and γ to some degree, it does not fully do so. In particular, if we set $\gamma = 0$, then $x_{t+1} = x_t$, in which case we can make no progress overall. This is particularly important because, as we show above, for many Θ , the only way for the surrogate loss to have the same critical point as the true loss is by setting $\gamma = 0$. More generally, we see that the effective learning rate used in such an update is actually the product $\eta\gamma$, which can result in conflating the effect of changes in γ with changes in η .

Appendix B. Proof of results

B.1 Results from Section 3

B.1.1 LEMMA 1

Proof Using the fact that A_z is symmetric for all z , we have

$$\begin{aligned}
 f_i(x) &= \mathbb{E}_{z \sim \mathcal{D}_i} [f(x; z)] \\
 &= \mathbb{E}_{z \sim \mathcal{D}_i} \left[\frac{1}{2} \|A_z^{1/2}(x - c_z)\|^2 \right] \\
 &= \mathbb{E}_{z \sim \mathcal{D}_i} \left[\frac{1}{2} (x - c_z)^T A_z (x - c_z) \right] \\
 &= \mathbb{E}_{z \sim \mathcal{D}_i} \left[\frac{1}{2} x^T A_z x - x^T A_z c_z + \frac{1}{2} c_z^T A_z c_z \right] \\
 &= \frac{1}{2} x^T \mathbb{E}_{z \sim \mathcal{D}_i} [A_z] x - x^T \mathbb{E}_{z \sim \mathcal{D}_i} [A_z c_z] + \frac{1}{2} \mathbb{E}_{z \sim \mathcal{D}_i} [c_z^T A_z c_z] \\
 &= \frac{1}{2} x^T A_i x - x^T A_i c_i + \frac{1}{2} \mathbb{E}_{z \sim \mathcal{D}_i} [c_z^T A_z c_z] \\
 &= \frac{1}{2} \|A_i^{1/2}(x - c_i)\|^2 - c_i^T A_i c_i + \frac{1}{2} \mathbb{E}_{z \sim \mathcal{D}_i} [c_z^T A_z c_z].
 \end{aligned}$$

Setting $\tau_i = -c_i^T A_i c_i + \frac{1}{2} \mathbb{E}_{z \sim \mathcal{D}_i} [c_z^T A_z c_z]$, we derive the result. ■

B.1.2 LEMMA 2

Proof For simplicity of notation, let $b_z = -A_z c_z$ and $b_i = -A_i c_i$. Let $S_{:k} = (S_1, S_2, \dots, S_k)$. By (5), g_k is independent of w_k given $S_{:k-1}$. Therefore, we have that for any k ,

$$\begin{aligned}
 \mathbb{E}[g_k] &= \mathbb{E}_{S_{:k-1}} \left[\mathbb{E}_{S_k} \left[\frac{1}{B} \sum_{z \in S_k} \nabla f(x_k; z) \middle| S_{:k-1} \right] \right] \\
 &= \mathbb{E}_{S_{:k-1}} \left[\mathbb{E}_{S_k} \left[\frac{1}{B} \sum_{z \in S_k} A_z x_k + b_z \middle| S_{:k-1} \right] \right] \\
 &= \mathbb{E}_{S_{:k-1}} [A_i x_k + b_i]
 \end{aligned}$$

By linearity of expectation, we then find that

$$\mathbb{E}[g_k] = A_i \mathbb{E}[x_k] + b_i. \quad (26)$$

By the assumption that A_i is positive definite, this implies

$$\mathbb{E}[x_k] = A_i^{-1} (\mathbb{E}[g_k] - b_i). \quad (27)$$

Plugging (27) into (6), we have

$$\mathbb{E}[x_{k+1}] = \mathbb{E}[x_k] - \gamma \mathbb{E}[g_k] = A_i^{-1}(\mathbb{E}[g_k] - b_i) - \gamma \mathbb{E}[g_k]. \quad (28)$$

Combining (26) and (27), we have

$$\begin{aligned} \mathbb{E}[g_{k+1}] &= A_i \mathbb{E}[x_{k+1}] + b_i \\ &= A_i (A_i^{-1}(\mathbb{E}[g_k] - b_i) - \gamma \mathbb{E}[g_k]) + b_i \\ &= (I - \gamma A_i) \mathbb{E}[g_k]. \end{aligned}$$

■

B.1.3 THEOREM 4

Proof For convenience of notation, we will fix i and let X_k denote $X_k^i(x)$, and let $X_0 = x$. Since we assume this is computed using gradient descent, we have

$$X_{k+1} = X_k - \gamma \nabla f_i(X_k).$$

Note that $\nabla^2 f_i(y) = A_i$ for all y . Therefore, for $0 \leq k \leq K-1$,

$$\nabla_{X_k} X_{k+1} = I - \gamma A_i. \quad (29)$$

Also recall that by Theorem 3, we have

$$\nabla_{X_K} f_i(X_K) = (I - \gamma A_i)^{K+1}. \quad (30)$$

For a function $q : \mathbb{R}^a \rightarrow \mathbb{R}^b$, let its Jacobian at a point $x \in \mathbb{R}^a$ be denoted by $J_x(q)$. Using the chain rule for Jacobians:

$$\begin{aligned} \nabla m_K^i(x) &= J_{X_K}(f_i(X_K)) J_x(X_K) \\ &= J_{X_K}(f_i(X_K)) \prod_{k=0}^{K-1} J_{X_k}(X_{k+1}) \\ &= (I - \gamma A_i)^{K+1} \prod_{k=1}^K (I - \gamma A_i). \end{aligned}$$

This last step follows from (29) and (30), and the fact that A_z is symmetric for all z . The remainder of the result follows directly from Theorem 3. ■

B.2 Results from Section 5

B.2.1 LEMMA 5

Proof By (8), we have

$$Q_i(0, \Theta) = \sum_{k=1}^{K(\Theta)} \theta_k (I - 0)^{k-1} = \left(\sum_{k=1}^{K(\Theta)} \theta_k \right) I.$$

Similarly, if $\Theta = (\theta_1)$ then

$$Q_i(\gamma, \Theta) = \theta_1 I.$$

In either event, we see that $Q_i(\gamma, \Theta) = aI$ where $a = \sum_{k=1}^{K(\Theta)} \theta_k$. Therefore,

$$\tilde{f}_i(x, \gamma, \Theta) = \frac{1}{2} \|(aA_i)^{1/2}(x - c_i)\|^2 = \frac{a}{2} \|A_i^{1/2}(x - c_i)\|^2 = a\tilde{f}_i(x, \gamma, \Theta).$$

■

B.2.2 LEMMA 6

Proof We prove each property below.

Proof of Property 1: Since $\gamma < L_i^{-1}$ and A_i is symmetric and positive definite we know that the matrix $I - \gamma A_i \succeq 0$ and therefore $(I - \gamma A_i)^k$ is symmetric and positive definite for all k . By (8) and Assumption 1, $Q_i(\gamma, \Theta)$ is a nonnegative linear combination of positive definite, symmetric matrices, with some coefficient $\theta_j > 0$. It is therefore positive definite and symmetric.

Proof of Property 2: Since $Q_i(\gamma, \Theta)$ and A_i are symmetric and positive definite, so too is their product. Therefore, the i -th surrogate loss defined in (9) is a positive definite quadratic function, and therefore has a unique minima. Solving for this minima explicitly by setting the gradient equal to 0, we get

$$\nabla_x \tilde{f}_i(x, \gamma, \Theta) = Q_i(\gamma, \Theta) A_i (x - c_i) = 0 \implies x = c_i.$$

Here, we again used the fact that $Q_i(\gamma, \Theta) A_i$ is symmetric and positive definite.

Proof of Property 3: Let v be an eigenvector of A_i with eigenvalue λ . Then note that v is an eigenvector of $(I - \gamma A_i)^{k-1}$ with eigenvalue $(1 - \gamma\lambda)^{k-1}$. Therefore, v is an eigenvector of $Q_i(\gamma, \Theta)$ with eigenvalue

$$\sum_{k=1}^{K(\Theta)} \theta_k (1 - \gamma\lambda)^{k-1}.$$

Proof of Property 4: This follows from Property 3, noting that since $\gamma < L_i^{-1}$, we have $\gamma\lambda < 1$ for all eigenvalues of A_i . By Property 3, the eigenvalue is maximized when $\lambda = \lambda_{\min}(A_i) = \mu_i$ and minimized when $\lambda = \lambda_{\max}(A_i) = L_i$. ■

B.2.3 LEMMA 10

Proof We prove each property below.

Proof of Property 1: This follows by analogous reasoning to Property 3 in Lemma 6. Note that every eigenvector v of A_i with associated eigenvalue λ is also an eigenvector of $(I - \gamma A_i)^{k-1}$ with eigenvalue $(1 - \gamma\lambda)^{k-1}$. By basic properties of eigenvectors, this implies the desired result.

Proof of Property 2: By Lemma 6, and because $\gamma < L_i^{-1} \leq \mu_i^{-1}$, for all $k \geq 1$,

$$0 < \lambda_{\min}((I - \gamma A_i)^{k-1}) = (1 - \gamma L_i)^{k-1} \leq (1 - \gamma \mu_i)^{k-1} = \lambda_{\max}((I - \gamma A_i)^{k-1}).$$

Since $(I - \gamma A_i)^{k-1}$ and A_i are positive definite, we have

$$\lambda_{\max}((I - \gamma A_i)^{k-1} A_i) \leq \lambda_{\max}((I - \gamma A_i)^{k-1}) \lambda_{\max}(A_i) = (1 - \gamma \mu_i)^{k-1} L_i.$$

Repeatedly using the fact that for Hermitian matrices, $\lambda_{\max}(A + B) \leq \lambda_{\max}(A) + \lambda_{\max}(B)$, we derive the upper bound on $\lambda_{\max}(Q_i(\gamma, \Theta) A_i)$. The lower bound on $\lambda_{\min}(Q_i(\gamma, \Theta) A_i)$ follows from a similar argument, using the fact that for Hermitian matrices, $\lambda_{\min}(A + B) \geq \lambda_{\min}(A) + \lambda_{\min}(B)$. \blacksquare

B.2.4 LEMMA 11

Proof

Proof of Property 1: This follows immediately from Property 1 of Lemma 10 and (18).

Proof of Property 2: Fix $\gamma < L_i$ and define

$$g(\lambda) := \phi_{K,\lambda}(\gamma).$$

Note that we have

$$g'(\lambda) = K(1 - \gamma\lambda)^{K-1}.$$

Since $\gamma < L_i^{-1}$, for $\lambda \in [\mu_i, L_i]$, we have $g'(\lambda) > 0$. Hence, for $\lambda \in [\mu_i, L_i]$ we know

$$g(\mu_i) \leq g(\lambda) \leq g(L_i).$$

Therefore, $g(\mu_i), g(L_i)$ are the minimum and maximum eigenvalues of $Q_i(\gamma, \Theta_{1:K}) A_i$.

Proof of Property 3: As in the proof of Property 2, for a fixed $\gamma < L^{-1}$ define

$$g(\lambda) := \phi_{K,\lambda}(\gamma).$$

Note that by assumption, we have $\gamma < L^{-1}$. Therefore, for $\lambda \in [\mu, L]$, $g'(\lambda) > 0$, so for all λ ,

$$g(\mu) \leq g(\lambda) \leq g(L).$$

This implies the desired result. \blacksquare

B.2.5 LEMMA 9

Proof Because $0 < \gamma < L_i^{-1}$, we have

$$0 \prec I - \gamma A_i \prec 1.$$

Therefore,

$$Q_i(\gamma, \Theta_{1:K}) = \sum_{k=1}^K (I - \gamma A_i)^{-1}$$

is a partial geometric sum of matrices with eigenvalues λ_i satisfying $0 < \lambda_i < 1$. This implies that, much like a geometric series of scalars,

$$Q_i(\gamma, \Theta_{1:K}) = (I - (I - \gamma A_i)^{-1})(\gamma A_i)^{-1}.$$

Note that here we used the fact that A_i commutes with $(I - \gamma A_i)$ to interchange their order. \blacksquare

B.2.6 LEMMA 12

Proof

Proof of Property 1: This follows immediately from Property 1 of Lemma 10 and (3).

Proof of Property 2: Fix $\gamma < (KL_i)^{-1}$ and define

$$g(\lambda) := (1 - \gamma\lambda)^{K-1}\lambda.$$

Note that we have

$$g'(\lambda) = (1 - \gamma\lambda)^{K-2}(1 - K\gamma\lambda).$$

Since $\gamma < (KL_i)^{-1}$, for $\lambda \in [\mu_i, L_i]$, we have

$$1 - K\gamma\lambda > 0.$$

In particular, this implies $1 - \gamma\lambda > 0$, so $g'(\lambda) > 0$. Hence, for $\lambda \in [\mu_i, L_i]$ we know

$$g(\mu_i) \leq g(\lambda) \leq g(L_i).$$

Therefore, $g(\mu_i), g(L_i)$ are the minimum and maximum eigenvalues of $Q_i(\gamma, \Theta_K)A_i$.

Proof of Property 3: As in the proof of Property 2, for a fixed $\gamma < L^{-1}$ define

$$g(\lambda) := (1 - \gamma\lambda)^{K-1}\lambda.$$

By assumption, $\gamma < L^{-1}$. Therefore, for $\lambda \in [\mu, L]$, $g'(\lambda) > 0$, so for such λ ,

$$g(\mu) \leq g(\lambda) \leq g(L).$$

This implies the desired result. ■

B.3 Results from Section 6

In order to prove the results in this section, we will use the following straightforward lemma regarding the structure of $x^*(\gamma, \Theta)$.

Lemma 30 *If $\gamma < L^{-1}$, then*

$$x^*(\gamma, \Theta) = \mathbb{E}[\tilde{A}_i]^{-1} \mathbb{E}[\tilde{A}_i c_i].$$

Proof By definition,

$$\tilde{f}(x, \gamma, \Theta) = \mathbb{E} \left[\frac{1}{2} \|(Q_i A_i)^{1/2} (x - c_i)\|^2 \right].$$

Therefore,

$$\nabla \tilde{f}(x, \gamma, \Theta) = \mathbb{E}[Q_i A_i (x - c_i)] = \mathbb{E}[Q_i A_i]x - \mathbb{E}[Q_i A_i c_i].$$

Since $\tilde{f}(x, \gamma, \Theta)$ is strongly convex, it then follows that

$$x^*(\gamma, \Theta) = \mathbb{E}_i[Q_i A_i]^{-1} \mathbb{E}_i[Q_i A_i c_i].$$

Scaling Q_i by $(\sum_k \theta_k)^{-1}$ in both parts of the right-hand side, we derive the result. ■

We will also need the following result on the relation between $\mathbb{E}[A^{-1}]$ and $\mathbb{E}[A]^{-1}$.

Lemma 31 (Groves and Rothenberg (1969)) *Let A be a random matrix such that A is always real, symmetric, and positive definite. Then*

$$\mathbb{E}[A]^{-1} \preceq \mathbb{E}[A^{-1}]$$

as long as all expectations exist.

In particular, this implies that for such a random matrix A , we have

$$\|\mathbb{E}[A]^{-1}\| \leq \|\mathbb{E}[A^{-1}]\|.$$

B.3.1 LEMMA 15

Proof We will first prove analogous statements for any $i \in \mathcal{I}$. Fix i, γ . By Lemma 11, we have

$$\tilde{f}_i(x, \gamma, \Theta_{1:K}) = \frac{1}{2} \|(Q_i(\gamma, \Theta_{1:K})A_i)^{1/2}(x - c_i)\|^2 \leq \frac{\phi_{K, L_i}(\gamma)}{2} \|x - c_i\|^2.$$

Since $0 < \gamma < L_i^{-1}$, by (17), we have $\phi_{K, L_i}(\gamma) \leq \gamma^{-1}$, implying that

$$\tilde{f}_i(x, \gamma, \Theta_{1:K}) \leq \frac{1}{2\gamma} \|x - c_i\|^2. \quad (31)$$

By Lemma 9, we have

$$Q_i(\gamma, \Theta_{1:K})A_i = \gamma^{-1}(I - (I - \gamma A_i)^K).$$

Since $0 \prec I - \gamma A_i \prec I$, this implies

$$\lim_{K \rightarrow \infty} Q_i(\gamma, \Theta_{1:K})A_i = \gamma^{-1}I. \quad (32)$$

Define

$$\tilde{f}_i^\infty(x, \gamma) := \frac{1}{2\gamma} \|x - c_i\|^2,$$

$$\tilde{f}^\infty(x, \gamma) := \mathbb{E}_{i \sim \mathcal{P}} [\tilde{f}_i^\infty(x, \gamma)].$$

Note that by Assumption 3, we know that $f^\infty(x, \gamma)$ is well-defined and finite at all $x \in \mathbb{R}^d$, as

$$\tilde{f}^\infty(x, \gamma) = \mathbb{E}_{i \sim \mathcal{P}} \left[\frac{1}{2} \|x - c_i\|^2 \right] \leq \mathbb{E}_{i \sim \mathcal{P}} \left[\|x - c\|^2 + \|c_i - c\|^2 \right] \leq \|x - c\|^2 + \sigma_c^2.$$

By (31), we have that for all K ,

$$\tilde{f}_i(x, \gamma, \Theta_{1:K}) \leq \tilde{f}_i^\infty(x, \gamma).$$

By (32), we have

$$\lim_{K \rightarrow \infty} \tilde{f}_i(x, \gamma, \Theta_{1:K}) = \tilde{f}_i^\infty(x, \gamma).$$

By the dominating convergence theorem, we have that for any x ,

$$\begin{aligned}
 \lim_{K \rightarrow \infty} \tilde{f}(x, \gamma, \Theta_{1:K}) &= \lim_{K \rightarrow \infty} \mathbb{E}_{i \sim \mathcal{P}} \tilde{f}_i(x, \gamma, \Theta_{1:K}) \\
 &= \mathbb{E}_{i \sim \mathcal{P}} \lim_{K \rightarrow \infty} \tilde{f}_i(x, \gamma, \Theta_{1:K}) \\
 &= \tilde{f}^\infty(x, \gamma) \\
 &= \frac{1}{2\gamma} \mathbb{E}_{i \sim \mathcal{P}} [\|x - c_i\|^2].
 \end{aligned}$$

The last part of the theorem follows from the fact that the expected value minimizes the expected ℓ_2 distance to a random point. \blacksquare

B.3.2 THEOREM 16

Proof Throughout this proof, we will use the fact that for a positive semi-definite, symmetric matrix P , $\|P\| = \lambda_{\max}(P)$ and that if P is further positive definite, $\|P^{-1}\| = \lambda_{\min}(P)^{-1}$.

By Lemma 30,

$$\begin{aligned}
 \|x^*(\gamma, \Theta) - x^*\| &= \|\mathbb{E}[\tilde{A}_i]^{-1} \mathbb{E}[\tilde{A}_i c_i] - \mathbb{E}[A_i]^{-1} \mathbb{E}[A_i c_i]\| \\
 &= \|\tilde{A}^{-1} \mathbb{E}[\tilde{A}_i c_i] - \mathbb{E}[c_i] + \mathbb{E}[c_i] - A^{-1} \mathbb{E}[A_i c_i]\| \\
 &= \|\tilde{A}^{-1} (\mathbb{E}[\tilde{A}_i c_i] - \mathbb{E}[\tilde{A}_i] \mathbb{E}[c_i]) - A^{-1} (\mathbb{E}[A_i c_i] - \mathbb{E}[A_i] \mathbb{E}[c_i])\| \\
 &= \|\tilde{A}^{-1} \tilde{v} - A^{-1} v\|.
 \end{aligned}$$

In the above, we defined

$$\begin{aligned}
 v &:= \mathbb{E}[A_i c_i] - \mathbb{E}[A_i] \mathbb{E}[c_i] \\
 \tilde{v} &:= \mathbb{E}[\tilde{A}_i c_i] - \mathbb{E}[\tilde{A}_i] \mathbb{E}[c_i].
 \end{aligned}$$

The vectors v and \tilde{v} measure the correlation between A_i (or \tilde{A}_i) and the c_i . When all A_i are equal, or all c_i are equal, one can easily show that $v = \tilde{v} = 0$. We then have

$$\begin{aligned}
 \|x^*(\gamma, \Theta) - x^*\| &= \|\tilde{A}^{-1}(\tilde{v} - v) + (\tilde{A}^{-1} - A^{-1})v\| \\
 &\leq \underbrace{\|\tilde{A}^{-1}\|}_{T_1} \underbrace{\|\tilde{v} - v\|}_{T_2} + \underbrace{\|\tilde{A}^{-1} - A^{-1}\|}_{T_3} \underbrace{\|v\|}_{T_4}.
 \end{aligned}$$

We first bound T_1 . Since Q_i and A_i are positive definite, so too is \tilde{A}_i and therefore \tilde{A} . We therefore have,

$$\begin{aligned}
 T_1 &= \|\tilde{A}^{-1}\| \\
 &= \|\mathbb{E}[\tilde{A}_i]^{-1}\| \\
 &\leq \|\mathbb{E}[\tilde{A}_i^{-1}]\| \\
 &\leq \mathbb{E}\|\tilde{A}_i^{-1}\| \\
 &= \mathbb{E}[\|A_i^{-1}(\tau Q_i)^{-1}\|] \\
 &\leq \mathbb{E}[\|A_i^{-1}\| \|(\tau Q_i)^{-1}\|] \\
 &\leq \mu^{-1} \mathbb{E}[\lambda_{\min}(\tau Q_i)^{-1}].
 \end{aligned}$$

For T_2 , we have the following:

$$\begin{aligned}
 T_2 &= \|\tilde{v} - v\| \\
 &= \|(\mathbb{E}[\tau Q_i A_i c_i] - \mathbb{E}[\tau Q_i A_i] \mathbb{E}[c_i]) - (\mathbb{E}[A_i c_i] - \mathbb{E}[A_i] \mathbb{E}[c_i])\| \\
 &= \|(\mathbb{E}[\tau Q_i A_i c_i] - \mathbb{E}[\tau Q_i A_i] c) - (\mathbb{E}[A_i c_i] - \mathbb{E}[A_i] c)\| \\
 &= \|\mathbb{E}[(\tau Q_i - I)(A_i c_i - A_i c)]\| \\
 &\leq \sqrt{\mathbb{E}[\|\tau Q_i - I\|^2] \mathbb{E}[\|A_i c_i - A_i c\|^2]} \\
 &\leq \sqrt{\mathbb{E}[\|\tau Q_i - I\|^2] \mathbb{E}[\|A_i\|^2 \|c_i - c\|^2]} \\
 &\leq L\sigma_c \sqrt{\mathbb{E}[\|\tau Q_i - I\|^2]}.
 \end{aligned}$$

For T_3 , we use the fact that for invertible matrices $B, C \in \mathbb{R}^{n \times n}$,

$$\|B^{-1} - C^{-1}\| = \|B^{-1}(B - C)C^{-1}\| \leq \|B^{-1}\| \|C^{-1}\| \|B - C\|.$$

Therefore,

$$T_3 \leq \|A^{-1}\| \|\tilde{A}^{-1}\| \|\tilde{A} - A\|.$$

Note that $\|\tilde{A}^{-1}\|$ is simply T_1 above, and that using a similar analysis, we have

$$\|A^{-1}\| \leq \mathbb{E}[\lambda_{\min}(A_i)^{-1}] \leq \mu^{-1}.$$

By the Cauchy-Schwarz inequality,

$$\begin{aligned}
 \|\tilde{A} - A\| &= \|\mathbb{E}[\tau Q_i A_i - A_i]\| \\
 &\leq \|\mathbb{E}[(\tau Q_i - I)A_i]\| \\
 &\leq \sqrt{\mathbb{E}[\|\tau Q_i - I\|^2] \mathbb{E}[\|A_i\|^2]} \\
 &\leq L\sqrt{\mathbb{E}[\|\tau Q_i - I\|^2]}.
 \end{aligned}$$

For T_4 , we again use the Cauchy-Schwarz inequality, as

$$\begin{aligned}
 T_4 &= \|\mathbb{E}[A_i c_i] - \mathbb{E}[A_i] \mathbb{E}[c_i]\| \\
 &= \|\mathbb{E}[(A_i - A)(c_i - c)]\| \\
 &\leq \sqrt{\mathbb{E}[\|A_i - A\|^2] \mathbb{E}[\|c_i - c\|^2]} \\
 &\leq \sigma_A \sigma_c.
 \end{aligned}$$

Putting this all together, we have

$$\|x^*(\gamma, \Theta) - x^*\| \leq \frac{L\sigma_c}{\mu} \left(1 + \frac{\sigma_A}{\mu}\right) \mathbb{E}[\lambda_{\min}(\tau Q_i)^{-1}] \sqrt{\mathbb{E}[\|\tau Q_i - I\|^2]}. \quad (33)$$

Note that by Assumption 2, we have that $1 - \gamma\mu \leq 1, 1 - \gamma L \leq 1$. By Lemma 6 and the definition of τ , this implies that for all i ,

$$0 \prec \tau Q_i \preceq I.$$

Therefore for all i ,

$$\|\tau Q_i - I\| = \lambda_{\max}(I - \tau Q_i) \leq 1 - \lambda_{\min}(\tau Q_i). \quad (34)$$

Combining (33) and (34), we have

$$\|x^*(\gamma, \Theta) - x^*\| \leq \frac{L\sigma_c}{\mu} \left(1 + \frac{\sigma_A}{\mu}\right) \frac{1 - \tau \min_i \{\lambda_{\min}(Q_i)\}}{\tau \min_i \{\lambda_{\min}(Q_i)\}}.$$

By Lemma 6 and Assumption 2, we find that for all i ,

$$\tau \lambda_{\min}(Q_i(\gamma, \Theta)) \geq \chi(\gamma, \Theta).$$

Therefore,

$$\frac{1 - \tau \min_i \{\lambda_{\min}(Q_i)\}}{\tau \min_i \{\lambda_{\min}(Q_i)\}} \leq \frac{1 - \chi(\gamma, \Theta)}{\chi(\gamma, \Theta)}.$$

■

B.3.3 THEOREM 17

Note that for $\Theta = \Theta_{1:K}$, the quantity τ defined in (19) is given by $\tau = K^{-1}$. We will require one further auxiliary lemma.

Lemma 32 *If $\gamma < L^{-1}$, then for all $i \in \mathcal{I}$ we have*

$$\|\tau Q_i(\gamma, \Theta_{1:K}) A_i - I\| \leq \frac{KL - \phi_{K,L}(\gamma)}{K}$$

where $\phi_{K,L}(\gamma)$ is as defined in (17).

Proof First note that since $\tau = K^{-1}$,

$$\|\tau Q_i(\gamma, \Theta_{1:K}) A_i - I\| = \frac{\|Q_i(\gamma, \Theta_{1:K}) A_i - KI\|}{K}.$$

It therefore suffices to show that

$$\|Q_i(\gamma, \Theta_{1:K}) A_i - KI\| \leq KL - \phi_{K,L}(\gamma).$$

As discussed in the proof of Lemma 10 and Lemma 11, $Q_i(\gamma, \Theta_{1:K}) A_i$ has eigenvalues of the form $\phi_{K,\lambda}(\gamma)$ where λ is an eigenvalue of A_i . Therefore, $KI - Q_i(\gamma, \Theta_{1:K}) A_i$ has eigenvalues of the form

$$q(\lambda) = K\lambda - \phi_{K,\lambda}(\gamma)$$

where λ is an eigenvalue of A_i . As noted in (18), for $\lambda\gamma \leq 1$,

$$\phi_{K,\lambda}(\gamma) = \sum_{k=1}^K (1 - \gamma\lambda)^{k-1} \lambda \leq K\lambda.$$

Therefore, $KI - Q_i(\gamma, \Theta_{1:K})A_i$ is symmetric and positive semi-definite. Moreover, a simple computation shows

$$q'(\lambda) = K - K(1 - \gamma\lambda)^{K-1}$$

which is nonnegative for $0 \leq \gamma\lambda \leq 1$. In particular it is nonnegative for $\gamma \in [0, L^{-1}]$ (as in Assumption 2), implying that

$$\lambda_{\max}(KI - Q_i(\gamma, \Theta_{1:K})A_i) \leq q(L) = KL - \phi_{K,L}(\gamma).$$

■

We can now prove the desired theorem.

Proof [Proof of Theorem 17] We begin our proof in a similar manner to the proof of Theorem 16. Note that for FedAvg with K local steps, $\tau = K$. By Lemma 30,

$$\begin{aligned} \|x^*(\gamma, \Theta_{1:K}) - x^*\| &= \|\mathbb{E}[\tilde{A}_i]^{-1} \mathbb{E}[\tilde{A}_i c_i] - \mathbb{E}[A_i]^{-1} \mathbb{E}[A_i c_i]\| \\ &= \|\tilde{A}^{-1} \mathbb{E}[\tilde{A}_i c_i] - \mathbb{E}[c_i] + \mathbb{E}[c_i] - A^{-1} \mathbb{E}[A_i c_i]\| \\ &= \|\tilde{A}^{-1} (\mathbb{E}[\tilde{A}_i c_i] - \mathbb{E}[\tilde{A}_i] \mathbb{E}[c_i]) - A^{-1} (\mathbb{E}[A_i c_i] - \mathbb{E}[A_i] \mathbb{E}[c_i])\| \\ &= \|\tilde{A}^{-1} \tilde{v} - A^{-1} v\|. \end{aligned}$$

In the above, we defined

$$\begin{aligned} v &:= \mathbb{E}[A_i c_i] - \mathbb{E}[A_i] \mathbb{E}[c_i] \\ \tilde{v} &:= \mathbb{E}[\tilde{A}_i c_i] - \mathbb{E}[\tilde{A}_i] \mathbb{E}[c_i]. \end{aligned}$$

We then have

$$\begin{aligned} \|x^*(\gamma, \Theta_{1:K}) - x^*\| &= \|\tilde{A}^{-1}(\tilde{v} - v) + (\tilde{A}^{-1} - A^{-1})v\| \\ &\leq \underbrace{\|\tilde{A}^{-1}\|}_{T_1} \underbrace{\|\tilde{v} - v\|}_{T_2} + \underbrace{\|\tilde{A}^{-1} - A^{-1}\|}_{T_3} \underbrace{\|v\|}_{T_4}. \end{aligned}$$

We first bound T_1 . Since Q_i and A_i are positive definite, so too is \tilde{A}_i and therefore \tilde{A} . We therefore have,

$$\begin{aligned} T_1 &= \|\tilde{A}^{-1}\| \\ &= \|\mathbb{E}[\tilde{A}_i]^{-1}\| \\ &\leq \|\mathbb{E}[\tilde{A}_i^{-1}]\| \\ &\leq \mathbb{E}\|\tilde{A}_i^{-1}\|. \end{aligned}$$

The penultimate step follows by Lemma 31. By definition of \tilde{A}_i^{-1} , we have

$$\begin{aligned} T_1 &\leq \mathbb{E}\|\tilde{A}_i^{-1}\| \\ &= K \mathbb{E}[\|(Q_i(\gamma, \Theta_{1:K})A_i)^{-1}\|] \\ &\leq K \phi_{K,\mu}(\gamma)^{-1}. \end{aligned}$$

Note that the last step follows by (17) and Lemma 11.

For T_2 , we have the following:

$$\begin{aligned}
 T_2 &= \|\tilde{v} - v\| \\
 &= \|(\mathbb{E}[\tau Q_i A_i c_i] - \mathbb{E}[\tau Q_i A_i] \mathbb{E}[c_i]) - (\mathbb{E}[A_i c_i] - \mathbb{E}[A_i] \mathbb{E}[c_i])\| \\
 &= \|(\mathbb{E}[\tau Q_i A_i c_i] - \mathbb{E}[\tau Q_i A_i] c) - (\mathbb{E}[A_i c_i] - \mathbb{E}[A_i] c)\| \\
 &= \|\mathbb{E}[(\tau Q_i(\gamma, \Theta_{1:K}) A_i - A_i)(c_i - c)]\| \\
 &\leq \sqrt{\mathbb{E}[\|\tau Q_i(\gamma, \Theta_{1:K}) A_i - A_i\|^2] \mathbb{E}[\|c_i - c\|^2]} \\
 &\leq \frac{\sigma_c(KL - \phi_{K,L}(\gamma))}{K}.
 \end{aligned}$$

This last step holds by Lemma 32 and Assumption 3.

For T_3 , we use the fact that for invertible matrices $B, C \in \mathbb{R}^{n \times n}$,

$$\|B^{-1} - C^{-1}\| = \|B^{-1}(B - C)C^{-1}\| \leq \|B^{-1}\| \|C^{-1}\| \|B - C\|.$$

Therefore,

$$T_3 \leq \|A^{-1}\| \|\tilde{A}^{-1}\| \|\tilde{A} - A\|.$$

Note that $\|\tilde{A}^{-1}\|$ is simply T_1 above, and that using a similar analysis, we have

$$\|A^{-1}\| \leq \mathbb{E}[\lambda_{\min}(A_i)^{-1}] \leq \mu^{-1}.$$

Again using Lemma 32,

$$\begin{aligned}
 \|\tilde{A} - A\| &= \|\mathbb{E}[\tau Q_i A_i - A_i]\| \\
 &\leq \mathbb{E}[\|(\tau Q_i - I)A_i\|] \\
 &\leq \frac{KL - \phi_{K,L}(\gamma)}{K}.
 \end{aligned}$$

For T_4 , we again use the Cauchy-Schwarz inequality, as

$$\begin{aligned}
 T_4 &= \|\mathbb{E}[A_i c_i] - \mathbb{E}[A_i] \mathbb{E}[c_i]\| \\
 &= \|\mathbb{E}[(A_i - A)(c_i - c)]\| \\
 &\leq \sqrt{\mathbb{E}[\|A_i - A\|^2] \mathbb{E}[\|c_i - c\|^2]} \\
 &\leq \sigma_A \sigma_c.
 \end{aligned}$$

Putting this all together, we have derive the result. ■

B.3.4 LEMMA 18

Proof By properties of geometric sums, we have

$$\phi_{K,\lambda}(\gamma) = \sum_{k=1}^K (1 - \gamma\lambda)^{k-1} \lambda.$$

Note that this implies that the function is differentiable everywhere. Taking a derivative, we have

$$\phi'_{K,\lambda}(\gamma) = \sum_{k=1}^K -(k-1)(1 - \gamma\lambda)^{k-2} \lambda^2.$$

Note that all terms in this sum are nonnegative when $\gamma \in [0, \lambda^{-1}]$. By assumption on ϵ , we have

$$\gamma \leq \frac{\ln(1/(1 - \epsilon))}{K\lambda} \leq \lambda^{-1}.$$

It therefore suffices to show the desired lower bound on $\phi_{K,\lambda}(\gamma)$ when

$$\gamma = \frac{\ln(1/(1 - \epsilon))}{K\lambda}.$$

By definition of $\phi_{K,\lambda}$, we have

$$\phi_{K,\lambda}(\gamma) = \frac{K\lambda}{\ln(1/(1 - \epsilon))} \left(1 - \left(1 - \frac{\ln(1/(1 - \epsilon))}{K} \right)^K \right).$$

Let $x = \ln(1/(1 - \epsilon))$. Note that by assumption on ϵ , $0 \leq x \leq 1$. It then suffices to show that

$$1 - \left(1 - \frac{x}{K} \right)^K \geq (1 - \epsilon)x$$

or equivalently,

$$\left(1 - \frac{x}{K} \right)^K \leq 1 - (1 - \epsilon)x. \tag{35}$$

By standard properties of exponentials,

$$\left(1 - \frac{x}{K} \right)^K \leq e^{-x} = e^{\ln(1-\epsilon)} = 1 - \epsilon.$$

Letting $y = 1 - \epsilon$, we then use the fact that for $y \in (0, 1]$,

$$y \leq 1 + y \ln(y) = 1 + (1 - \epsilon) \ln(1 - \epsilon) = 1 - (1 - \epsilon) \ln(1/(1 - \epsilon)).$$

This implies (35), proving the result. ■

B.3.5 THEOREM 21

We will first require an auxiliary lemma.

Lemma 33 *Suppose $\gamma_1 \leq \gamma_2 \leq L^{-1}$ and Assumption 2 holds. Then for all i , the matrix*

$$C = Q_i(\gamma_1, \Theta_{1:K})A_i - Q_i(\gamma_2, \Theta_{1:K})A_i$$

is positive semidefinite and satisfies

$$\lambda_{\max}(C) \leq \phi_{K,L}(\gamma_1) - \phi_{K,L}(\gamma_2).$$

Proof Recall that by Lemma 11, the eigenvalues of $Q_i(\gamma, \Theta)A_i$ are of the form

$$\gamma^{-1}(1 - (1 - \gamma\lambda)^K).$$

We define a function

$$h(\lambda) := \gamma_1^{-1}(1 - (1 - \gamma_1\lambda)^K) - \gamma_2^{-1}(1 - (1 - \gamma_2\lambda)^K).$$

Since $Q_i(\gamma_1, \Theta_{1:K})A_i$ and $Q_i(\gamma_2, \Theta_{1:K})A_i$ share the same eigenvectors as A_i , the eigenvalues of C are of the form $h(\lambda)$ where λ is an eigenvalue of A_i . Since $\gamma_1 \leq \gamma_2 < L_i^{-1}$, we clearly have $h(\lambda) \geq 0$ for $\lambda \in [\mu_i, L_i]$, implying that C is positive semidefinite.

For the maximum eigenvalue of C , we consider $h'(\lambda)$. A simple calculation shows

$$h'(\lambda) = K(1 - \gamma_1\lambda)^{K-1} - K(1 - \gamma_2\lambda)^{K-1}.$$

Since $\gamma_1 \leq \gamma_2 < L^{-1}$, we find that $h'(\lambda) \geq 0$ for $\lambda \in [0, L]$. Therefore, the maximum eigenvalue of C satisfies

$$\lambda_{\max}(C) \leq h(L) = \phi_{K,L}(\gamma_1) - \phi_{K,L}(\gamma_2).$$

■

We can now use this to prove the desired result, in a manner similar to the proof of Theorem 17.

Proof [Proof of Theorem 21] For notational convenience, we define the following quantities (where $i \in \mathcal{I}, j \in \{1, 2\}$)

$$\begin{aligned} B_{i,j} &:= \tau Q_i(\gamma_j, \Theta_{1:K})A_i \\ B_j &:= \mathbb{E}_i[B_{i,j}] \\ v_j &:= \mathbb{E}[B_{i,1}c_i] - \mathbb{E}[B_{i,j}] \mathbb{E}[c_i] \end{aligned}$$

By Lemma 30, we know

$$\begin{aligned} \|x^*(\gamma_1, \Theta_{1:K}) - x^*(\gamma_2, \Theta_{1:K})\| &= \|B_1^{-1} \mathbb{E}[B_{i,1}c_i] - B_2^{-1} \mathbb{E}[B_{i,2}c_i]\| \\ &= \|B_1^{-1} \mathbb{E}[B_{i,1}c_i] - \mathbb{E}[c_i] + \mathbb{E}[c_i] - B_2^{-1} \mathbb{E}[B_{i,2}c_i]\| \\ &= \|B_1^{-1}v_1 - B_2^{-1}v_2\|. \end{aligned}$$

Splitting this up, we get

$$\begin{aligned} \|x^*(\gamma_1, \Theta_{1:K}) - x^*(\gamma_2, \Theta_{1:K})\| &= \|B_1^{-1}(v_1 - v_2) + (B_1^{-1} - B_2^{-1})v_2\| \\ &\leq \underbrace{\|B_1^{-1}\|}_{T_1} \underbrace{\|v_1 - v_2\|}_{T_2} + \underbrace{\|B_1^{-1} - B_2^{-1}\|}_{T_3} \underbrace{\|v_2\|}_{T_4}. \end{aligned}$$

As in the proof of Theorem 16, we can use the fact that $Q_i(\gamma_1, \Theta)$ and A_i are symmetric and positive definite to bound T_1 , as we have

$$\begin{aligned} T_1 &= \|B_1^{-1}\| \\ &= \|\mathbb{E}[B_{1,i}]^{-1}\| \\ &\leq \|\mathbb{E}[B_{1,i}^{-1}]\| \\ &\leq \mathbb{E}\|B_{1,i}^{-1}\|. \end{aligned}$$

The penultimate step follows by Lemma 31. By definition of $B_{1,i}^{-1}$,

$$\begin{aligned} T_1 &\leq \mathbb{E}\|B_{1,i}^{-1}\| \\ &= \mathbb{E}\|(K^{-1}Q_i(\gamma_1, \Theta_{1:K})A_i)^{-1}\| \\ &\leq K\lambda_{\min}(Q_i(\gamma_1, \Theta_{1:K})A_i)^{-1} \\ &\leq K\phi_{K,\mu}(\gamma_1)^{-1}. \end{aligned}$$

This last step follows directly from Lemma 11.

For T_2 , we have the following:

$$\begin{aligned} T_2 &= \|v_1 - v_2\| \\ &= \|(\mathbb{E}[B_{i,1}c_i] - \mathbb{E}[B_{1,i}]\mathbb{E}[c_i]) - (\mathbb{E}[B_{i,2}c_i] - \mathbb{E}[B_{i,2}]\mathbb{E}[c_i])\| \\ &= \|(\mathbb{E}[B_{i,1}c_i] - \mathbb{E}[B_{1,i}]c) - (\mathbb{E}[B_{i,2}c_i] - \mathbb{E}[B_{i,2}]c)\| \\ &= \|\mathbb{E}[(B_{i,1} - B_{i,2})c_i - (B_{i,1} - B_{i,2})c]\| \\ &= \|\mathbb{E}[(B_{i,1} - B_{i,2})(c_i - c)]\| \\ &\leq \sqrt{\mathbb{E}[\|B_{i,1} - B_{i,2}\|^2] \mathbb{E}[\|c_i - c\|^2]} \\ &\leq \sigma_c \sqrt{\mathbb{E}[\|B_{i,1} - B_{i,2}\|^2]}. \end{aligned}$$

By definition of $B_{i,j}$, we have

$$\begin{aligned} \|B_{i,1} - B_{i,2}\| &= \|K^{-1}Q_i(\gamma_1, \Theta_{1:K})A_i - K^{-1}Q_i(\gamma_2, \Theta_{1:K})A_i\| \\ &\leq K^{-1}\|Q_i(\gamma_1, \Theta_{1:K})A_i - Q_i(\gamma_2, \Theta_{1:K})A_i\| \\ &\leq K^{-1}(\phi_{K,L}(\gamma_1) - \phi_{K,L}(\gamma_2)). \end{aligned}$$

Here, this last step follows from Lemma 33.

For T_3 , we use the fact that for invertible matrices $A, B \in \mathbb{R}^{n \times n}$,

$$\|A^{-1} - B^{-1}\| = \|A^{-1}(A - B)B^{-1}\| \leq \|A^{-1}\| \|B^{-1}\| \|A - B\|.$$

Therefore,

$$T_3 \leq \|B_1^{-1}\| \|B_2^{-1}\| \|B_1 - B_2\|.$$

Note that $\|B_j^{-1}\|$ can be bounded in the same manner as T_1 above. For the remaining term, we have

$$\begin{aligned} \|B_1 - B_2\| &= K^{-1} \|\mathbb{E}[Q_i(\gamma_1, \Theta_{1:K})A_i - Q_i(\gamma_2, \Theta_{1:K})A_i]\| \\ &\leq K^{-1} \mathbb{E}\|Q_i(\gamma_1, \Theta_{1:K})A_i - Q_i(\gamma_2, \Theta_{1:K})A_i\| \\ &\leq K^{-1}(\phi_{K,L}(\gamma_1) - \phi_{K,L}(\gamma_2)). \end{aligned}$$

This last step follows from Lemma 33.

Finally, for T_4 we have

$$\begin{aligned} T_4 &= \|\mathbb{E}[B_{i,2}c_i] - \mathbb{E}[B_{i,2}] \mathbb{E}[c_i]\| \\ &= \|\mathbb{E}[(B_{i,2} - B_2)(c_i - c)]\| \\ &\leq \sqrt{\mathbb{E}[\|B_{i,2} - B_2\|^2] \mathbb{E}[\|c_i - c\|^2]} \\ &\leq \sigma_c \sqrt{\mathbb{E}[\|B_{i,2} - B_2\|^2]} \\ &\leq \sigma_c \sqrt{\mathbb{E}[\|B_{i,2}\|^2]}. \end{aligned}$$

By Lemma 11, we have that for all i ,

$$\|B_{i,2}\| = \|\tau Q_i(\gamma_2, \Theta_{1:K})A_i\| = \frac{\phi_{K,L}(\gamma_2)}{K}$$

therefore implying that

$$T_4 \leq \sigma_c \frac{\phi_{K,L}(\gamma_2)}{K}.$$

Putting this all together, we find

$$\begin{aligned} \|x^*(\gamma_1, \Theta_{1:K}) - x^*(\gamma_2, \Theta_{1:K})\| &\leq T_1 T_2 + T_3 T_4 \\ &\leq \sigma_c \left(1 + \frac{\phi_{K,L}(\gamma_2)}{\phi_{K,\mu}(\gamma_2)}\right) \left(\frac{\phi_{K,L}(\gamma_1) - \phi_{K,L}(\gamma_2)}{\phi_{K,\mu}(\gamma_1)}\right). \end{aligned}$$

■

B.3.6 COROLLARY 22

To prove this, we will need to first bound the term $\phi_{K,L}(\gamma)/\phi_{K,\mu}(\gamma)$. To do so, we first require a simple lemma regarding ratios of sums.

Lemma 34 *For $n \geq 1$, let $a_1, \dots, a_n, b_1, \dots, b_n$ be positive real numbers such that for $1 \leq i \leq n$,*

$$\frac{a_i}{b_i} \leq c.$$

Then

$$\frac{a_1 + \dots + a_n}{b_1 + \dots + b_n} \leq c.$$

Proof We will prove this inductively. Note that when $n = 1$, the result immediately follows by assumption.

For $n > 1$, applying the inductive hypothesis to $a_1 + \dots + a_{n-1}$, we have

$$\frac{a_1 + \dots + a_n}{b_1 + \dots + b_n} \leq \frac{c(b_1 + \dots + b_{n-1}) + a_n}{b_1 + \dots + b_n}$$

Let $x = c(b_1 + \dots + b_{n-1})$, $y = b_1 + \dots + b_{n-1}$. Note that $x/y \leq c$, so applying the inductive hypothesis we have

$$\begin{aligned} \frac{a_1 + \dots + a_n}{b_1 + \dots + b_n} &\leq \frac{c(b_1 + \dots + b_{n-1}) + a_n}{b_1 + \dots + b_n} \\ &= \frac{x + a_n}{y + b_n} \\ &\leq c. \end{aligned}$$

■

We can now derive a bound on the condition number $\phi_{K,L}(\gamma)/\phi_{K,\mu}(\gamma)$.

Lemma 35 For $\mu \leq L$, $\gamma \in [0, L^{-1}]$ and $K \geq 1$,

$$\frac{\phi_{K,L}(\gamma)}{\phi_{K,\mu}(\gamma)} \leq \frac{L}{\mu}. \quad (36)$$

Proof For $1 \leq j \leq K$, define

$$a_j := (1 - \gamma L)^{j-1} L,$$

$$b_j := (1 - \gamma \mu)^{j-1} \mu.$$

Since $\mu \leq L$, $(1 - \gamma L) \leq (1 - \gamma \mu)$. Therefore,

$$\frac{a_i}{b_i} = \frac{L (1 - \gamma L)^{i-1}}{\mu (1 - \gamma \mu)^{i-1}} \leq \frac{L}{\mu}.$$

Applying Lemma 34, we have

$$\frac{a_1 + \dots + a_K}{b_1 + \dots + b_K} \leq \frac{L}{\mu}.$$

The proof then follows by noting that

$$\phi_{K,L}(\gamma) = a_1 + \dots + a_K$$

and

$$\phi_{K,\mu}(\gamma) = b_1 + \dots + b_K.$$

■

With this in hand, we can prove Corollary 22.

Proof [Proof of Corollary 22] By definition of $\phi_{K,L}$, we have

$$\begin{aligned}
 \phi_{K,L}(\gamma_1) - \phi_{K,L}(\gamma_2) &= \sum_{k=1}^K (1 - \gamma_1 L)^{k-1} L - (1 - \gamma_2 L)^{k-1} L \\
 &= \sum_{k=2}^K (1 - \gamma_1 L)^{k-1} L - (1 - \gamma_2 L)^{k-1} L \\
 &\leq \sum_{k=2}^K (1 - \gamma_1 L)^{k-1} L - (1 - \gamma_2 L)(1 - \gamma_1 L)^{k-2} L \\
 &= \sum_{k=2}^K (1 - \gamma_1 L)^{k-2} L ((1 - \gamma_1 L) - (1 - \gamma_2 L)) \\
 &= \left(\sum_{k=2}^K (1 - \gamma_1 L)^{k-2} L \right) L(\gamma_2 - \gamma_1).
 \end{aligned}$$

Here the second line follows from the fact that $(1 - \gamma_1 L)^0 = (1 - \gamma_2 L)^0 = 1$, and the third line follows from the fact that $\gamma_1 \leq \gamma_2$. Therefore,

$$\begin{aligned}
 \phi_{K,L}(\gamma_1) - \phi_{K,L}(\gamma_2) &\leq \left(\sum_{k=2}^K (1 - \gamma_1 L)^{k-2} L \right) L(\gamma_2 - \gamma_1) \\
 &\leq \phi_{K,L}(\gamma_1) L(\gamma_2 - \gamma_1).
 \end{aligned}$$

By Theorem 21, this implies

$$\|x^*(\gamma_1, \Theta_{1:K}) - x^*(\gamma_2, \Theta_{1:K})\| \leq \sigma_c \left(1 + \frac{\phi_{K,L}(\gamma_2)}{\phi_{K,\mu}(\gamma_2)} \right) \frac{\phi_{K,L}(\gamma_1)}{\phi_{K,\mu}(\gamma_1)} L(\gamma_2 - \gamma_1).$$

The result follows by applying Lemma 35 and noting that $L \geq \mu$. ■

B.4 Results in Section 7

B.4.1 LEMMA 23

Proof Recall that in Algorithm 1,

$$q_\gamma(x) = \frac{1}{M} \sum_{i \in \mathcal{I}} q^i$$

where $q^i = \text{InnerLoop}(i, x, \gamma, \Theta)$ (Algorithm 2) and \mathcal{I} is a set of size M sampled independently and uniformly at random from \mathcal{P} . Since the q^i are independent, it suffices to show that for any i , the vector $q^i := \text{InnerLoop}(i, x, \gamma, \Theta)$ satisfies

$$\mathbb{E} \|q^i - \mathbb{E}[q^i]\|^2 \leq \frac{KG^2}{B}.$$

By Algorithm 2, we have

$$q^i = \sum_{k=1}^K g_k$$

where g_k is a mini-batch stochastic gradient of batch size B taken at x_k , and the x_k are updated via

$$x_{k+1} = x_k - \gamma g_k.$$

Let $s_k = g_k - \mathbb{E}[g_k]$, and let $s_{1:k} = s_1 + \dots + s_k$. Note that $\{s_{1:k}\}_{k=1}^K$ form a Martingale sequence. We therefore have

$$\mathbb{E}\|q^i - \mathbb{E}[q^i]\|^2 = \mathbb{E}\|s_{1:k}\|^2 = \sum_{k=1}^K \mathbb{E}\|s_{1:k}\|^2.$$

By Assumption 4, we have that for any k and $z \sim \mathcal{D}_i$,

$$\mathbb{E}\|\nabla f(x_k; z) - \mathbb{E}[\nabla f(x_k; z)]\| \leq G^2.$$

Since

$$s_k = \frac{1}{B} \sum_{z \in S_k} \nabla f(x_k; z) - \mathbb{E}[\nabla f(x_k; z)]$$

where $|S_k| = B$ and each $z \in S_k$ is identically and independently distributed, we have

$$\mathbb{E}\|s_k\|^2 \leq \frac{G^2}{B}$$

implying from our reasoning above that $\mathbb{E}\|s_{1:k}\|^2 \leq KG^2/B$, therefore implying the desired result on the variance of q_t . \blacksquare

B.4.2 LEMMA 25

Proof We will proceed using a similar analysis to Lemma 1 in Rakhlin et al. (2012).

Since \tilde{f}_γ is μ_γ strongly convex (by Lemma 24), we have

$$\langle \nabla \tilde{f}_\gamma(x_t), x_t - x_\gamma^* \rangle \geq \tilde{f}_\gamma(x_t) - \tilde{f}_\gamma^* + \frac{\mu_\gamma}{2} \|x_t - x_\gamma^*\|^2, \quad (37)$$

$$\tilde{f}_\gamma(x_t) - \tilde{f}_\gamma^* \geq \frac{\mu_\gamma}{2} \|x_t - x_\gamma^*\|^2. \quad (38)$$

Since \tilde{f}_γ is L_γ smooth, we have

$$\|\nabla \tilde{f}_\gamma(x)\| \leq L_\gamma \|x - x_\gamma^*\|. \quad (39)$$

Let $q_t := q_\gamma(x_t)$. Recall that we have

$$x_{t+1} = x_t - \eta_t q_t$$

and

$$\mathbb{E}[q_t] = \nabla \tilde{f}_\gamma(x_t).$$

Using the equations (37) and (38), we have

$$\begin{aligned} & \mathbb{E}[\|x_{t+1} - x_\gamma^*\|^2] \\ &= \mathbb{E}[\|x_t - \eta_t q_t - x_\gamma^*\|^2] \\ &= \mathbb{E}[\|x_t - x_\gamma^*\|^2 - 2\eta_t \mathbb{E}[\langle q_t, x_t - x_\gamma^* \rangle] + \eta_t^2 \mathbb{E}[\|q_t\|^2]] \\ &\leq \mathbb{E}[\|x_t - x_\gamma^*\|^2 - 2\eta_t \mathbb{E}[\langle q_t, x_t - x_\gamma^* \rangle] + \eta_t^2 \mathbb{E}[\|q_t\|^2]] \\ &= \mathbb{E}[\|x_t - x_\gamma^*\|^2 - 2\eta_t \mathbb{E}[\langle \nabla \tilde{f}_\gamma(x_t), x_t - x_\gamma^* \rangle] + \eta_t^2 \mathbb{E}[\|q_t\|^2]] \\ &\leq \mathbb{E}[\|x_t - x_\gamma^*\|^2 - 2\eta_t \mathbb{E}[\tilde{f}_\gamma(x_t) - \tilde{f}_\gamma^* + \frac{\mu_\gamma}{2} \|x_t - x_\gamma^*\|^2] + \eta_t^2 \mathbb{E}[\|q_t\|^2]] \\ &\leq \mathbb{E}[\|x_t - x_\gamma^*\|^2 - 2\eta_t \mathbb{E}[\frac{\mu_\gamma}{2} \|x_t - x_\gamma^*\|^2 + \frac{\mu_\gamma}{2} \|x_t - x_\gamma^*\|^2] + \eta_t^2 \mathbb{E}[\|q_t\|^2]] \\ &= (1 - 2\eta_t \mu_\gamma) \mathbb{E}[\|x_t - x_\gamma^*\|^2] + \eta_t^2 \mathbb{E}[\|q_t\|^2]. \end{aligned}$$

Applying Lemma 23, (39) and (22), we have

$$\begin{aligned} & \mathbb{E}[\|x_{t+1} - x_\gamma^*\|^2] \\ &\leq (1 - 2\eta_t \mu_\gamma) \mathbb{E}\|x_t - x_\gamma^*\|^2 + \eta_t^2 \mathbb{E}[\|q_t\|^2] \\ &\leq (1 - 2\eta_t \mu_t) \mathbb{E}[\|x_t - x_\gamma^*\|^2] + \eta_t^2 \mathbb{E}[\|\nabla \tilde{f}_\gamma(x_t)\|^2] + \eta_t^2 \frac{KG^2}{MB} \\ &\leq (1 - 2\eta_t \mu_\gamma + \eta_t^2 L_\gamma^2) \mathbb{E}\|x_t - x_\gamma^*\|^2 + \eta_t^2 \frac{KG^2}{MB} \\ &\leq (1 - \eta_t \mu_\gamma) \mathbb{E}\|x_t - x_\gamma^*\|^2 + \eta_t^2 \frac{KG^2}{MB}. \end{aligned}$$

■

B.4.3 THEOREM 27

Proof We will proceed using similar techniques to those in Theorem 4.7 of Bottou et al. (2018). Note that by construction of b_γ, a_γ , we have that for all $t \geq 1$,

$$\eta_t \leq \frac{a_\gamma}{b_\gamma} = \frac{\mu_\gamma}{L_\gamma^2}.$$

Therefore, by Lemma 25,

$$\mathbb{E}[\|x_{t+1} - x_\gamma^*\|^2] \leq (1 - \eta_t \mu_\gamma) \mathbb{E}[\|x_t - x_\gamma^*\|^2] + \eta_t^2 \frac{KG^2}{MB}. \quad (40)$$

We then proceed by induction. For $t = 1$, we have

$$\|x_1 - x_\gamma^*\|^2 = \frac{(b_\gamma + 1)\|x_1 - x_\gamma^*\|^2}{b_\gamma + 1} \leq \frac{v_\gamma}{b_\gamma + 1}.$$

For $t > 1$, let $\hat{t} := b_\gamma + t$. Therefore, $\eta_t = a_\gamma/\hat{t}$. Using (40) and the inductive hypothesis,

$$\begin{aligned} \mathbb{E}[\|x_{t+1} - x_\gamma^*\|^2] &\leq \left(1 - \frac{a_\gamma \mu_\gamma}{\hat{t}}\right) \frac{\nu_\gamma}{\hat{t}} + \frac{a_\gamma^2 K G^2}{\hat{t}^2 M B} \\ &= \left(\frac{\hat{t} - 2}{\hat{t}^2}\right) \nu_\gamma + \frac{4K G^2}{\mu_\gamma^2 \hat{t}^2 M B} \\ &= \left(\frac{\hat{t} - 1}{\hat{t}^2}\right) \nu_\gamma - \frac{\nu_\gamma}{\hat{t}^2} + \frac{4K G^2}{\mu_\gamma^2 \hat{t}^2 M B} \\ &= \left(\frac{\hat{t} - 1}{\hat{t}^2}\right) \nu_\gamma + \underbrace{\frac{1}{\hat{t}^2} \left(-\nu_\gamma + \frac{4K G^2}{\mu_\gamma^2 M B}\right)}_{\Xi} \end{aligned}$$

Note that $\Xi \leq 0$ by assumption on ν_γ , and that simple analysis shows

$$\hat{t}^2 \geq (\hat{t} - 1)(\hat{t} + 1).$$

Putting this together, we have

$$\mathbb{E}[\|x_{t+1} - x_\gamma^*\|^2] \leq \frac{\nu_\gamma}{\hat{t} + 1} = \frac{\nu_\gamma}{b_\gamma + t + 1}.$$

■

B.4.4 COROLLARY 28

Proof We have

$$\mathbb{E}[\|x_t - x^*\|^2] \leq 2 \mathbb{E}[\|x_t - x_\gamma^*\|^2] + 2 \|x_\gamma^* - x^*\|^2.$$

Using the bounds in Theorems 27 and Corollary 20, we have

$$\mathbb{E}[\|x_t - x^*\|^2] \leq \frac{2\nu_\gamma}{b_\gamma + t} + 2\sigma_c^2 \left(1 + \frac{\sigma_a}{\mu}\right)^2 \frac{L^2}{\mu^2} \frac{\epsilon^2}{(1 - \epsilon)^2}$$

where

$$\nu_\gamma := \max \left\{ \frac{4K G^2}{\mu_\gamma^2 M B}, (b_\gamma + 1) \|x_1 - x_\gamma^*\|^2 \right\}.$$

By Lemma 18 and assumption on γ, ϵ , we have

$$\frac{1}{\mu_\gamma} \leq \frac{1}{(1 - \epsilon) K \mu}.$$

Using this to derive an upper bound on the first term in ν_γ , we conclude the proof. ■

B.4.5 THEOREM 29

For convenience of notation (and in a slight abuse of previous notation), we define

$$\begin{aligned}\mu_t &:= \phi_{K,\mu}(\gamma_t) \\ L_t &:= \phi_{K,L}(\gamma_t) \\ \tilde{f}_t(x) &:= \tilde{f}(x, \gamma_t, \Theta_{1:K}) \\ x_t^* &:= \arg \min_x \tilde{f}_t(x) \\ \kappa &:= L/\mu.\end{aligned}$$

Proof We have

$$\begin{aligned}\mathbb{E}[\|x_t - x^*\|^2] &= \mathbb{E}[\|x_t - x_t^* + x_t^* - x^*\|^2] \\ &\leq 2 \underbrace{\mathbb{E}[\|x_t - x_t^*\|^2]}_{\alpha_t} + 2 \underbrace{\|x_t^* - x^*\|^2}_{\beta_t}.\end{aligned}$$

Next, note that for any $t \geq 1$,

$$\eta_t = \frac{a_t}{b+t} = \frac{2/\mu_t}{2\kappa^2+t} < \frac{1}{\mu_t\kappa^2}.$$

Note that by Lemma 35 we have

$$\frac{L_t}{\mu_t} \leq \frac{L}{\mu} = \kappa.$$

Therefore,

$$\eta_t \leq \frac{1}{\mu_t\kappa^2} \leq \frac{\mu_t^2}{\mu_t L_t^2} = \frac{\mu_t}{L_t^2}.$$

Therefore, we can apply Lemma 25 (with $\mu_\gamma = \mu_t, L_\gamma = L_t, x_\gamma^* = x_t^*$) to find

$$\mathbb{E}[\|x_{t+1} - x_t^*\|^2] \leq (1 - \eta_t\mu_t) \mathbb{E}[\|x_t - x_t^*\|^2] + \eta_t^2 \frac{KG^2}{MB}. \quad (41)$$

For any $\omega_t > 0$, we therefore have

$$\mathbb{E}[\|x_{t+1} - x_t^*\|^2] \leq (1 + \omega_t) \left(\mathbb{E}[\|x_{t+1} - x_t^*\|^2] \right) + (1 + \omega_t^{-1}) \|x_t^* - x_{t+1}^*\|^2. \quad (42)$$

Using (41), we derive the following recursion on the α_t .

$$\alpha_{t+1} \leq (1 + \omega_t) \left((1 - \eta_t\mu_t)\alpha_t + \eta_t^2 \frac{KG^2}{MB} \right) + (1 + \omega_t^{-1}) \|x_t^* - x_{t+1}^*\|^2. \quad (43)$$

Let $C = 4\sigma_c^2\kappa^2$ and let $\hat{t} = b + t$. . We will use (43) inductively to show that

$$\alpha_t \leq \frac{\nu + C}{\hat{t}}. \quad (44)$$

For $t = 1$, we have

$$\alpha_1 = \|x_1 - x_1^*\|^2 = \frac{(b+1)\|x_1 - x_1^*\|^2}{b+1} \leq \frac{\nu_1}{b+1}. \quad (45)$$

Similar analysis can be done in the case that $t = 2$. When $t \geq 3$, using the inductive hypothesis, we have

$$\begin{aligned} (1 - \eta_t \mu_t) \alpha_t + \eta_t^2 \frac{KG^2}{MB} &\leq (1 - \eta_t \mu_t) \frac{\nu + C}{\hat{t}} + \frac{a_t^2 KG^2}{\hat{t}^2 MB} \\ &\leq \left(\frac{\hat{t} - 3}{\hat{t}^2} \right) (\nu + C) + \frac{9KG^2}{\mu_t^2 \hat{t}^2 MB} \\ &= \left(\frac{\hat{t} - 2}{\hat{t}^2} \right) (\nu + C) - \frac{C}{\hat{t}^2} + \frac{1}{\hat{t}^2} \underbrace{\left(-\nu + \frac{9KG^2}{\mu_t^2 MB} \right)}_{\xi_t}. \end{aligned}$$

By definition of ν , we have

$$\xi_t \leq \frac{9KG^2}{\mu_t^2 MB} - \frac{18G^2}{\mu^2 KMB}.$$

However, since $\gamma_t \leq \ln(2)/K\mu$, by Lemma 18, we know

$$\mu_t \geq \frac{K\mu}{2}.$$

Therefore,

$$\xi_t \leq \frac{18G^2}{\mu^2 KMB} - \frac{18G^2}{\mu^2 KMB} = 0.$$

Hence,

$$(1 - \eta_t \mu_t) \alpha_t + \eta_t^2 \frac{KG^2}{MB} \leq \left(\frac{\hat{t} - 2}{\hat{t}^2} \right) (\nu + C) - \frac{C}{\hat{t}^2}. \quad (46)$$

Let

$$\omega_t = \frac{\hat{t} + 2}{(\hat{t} - 2)(\hat{t} + 1)}.$$

Note that this implies that

$$1 + \omega_t = \frac{\hat{t}^2}{(\hat{t} - 2)(\hat{t} + 1)}$$

and

$$1 + \omega_t^{-1} = \frac{\hat{t}^2}{\hat{t} + 2}.$$

Therefore, multiplying (46) by $1 + \omega_t$, we have

$$(1 + \omega_t) \left((1 - \eta_t \mu_t) \alpha_t + \eta_t^2 \frac{KG^2}{MB} \right) \leq \frac{\nu + C}{\hat{t} + 1} - \frac{C}{(\hat{t} - 2)(\hat{t} + 1)}. \quad (47)$$

This bounds the first part of (43). For the second part, we will use Corollary 22. In particular, since

$$\gamma_t \leq \frac{1}{L\hat{t}}$$

we find that

$$\begin{aligned} \|x_t^* - x_{t+1}^*\|^2 &\leq 4\sigma_c^2\kappa^4 \left(\frac{1}{\hat{t}} - \frac{1}{\hat{t}+1} \right)^2 \\ &= \frac{C\kappa^2}{\hat{t}^2(\hat{t}+1)^2} \\ &\leq \frac{C}{\hat{t}^2(\hat{t}+1)}. \end{aligned}$$

Here we used the fact that $\hat{t} + 1 \geq b \geq \kappa^2$. Multiplying by $1 + \omega_t^{-1}$,

$$(1 + \omega_t^{-1})\|x_t^* - x_{t+1}^*\|^2 \leq \frac{C}{(\hat{t}+1)(\hat{t}+2)}. \quad (48)$$

Combining (43), (47) and (48), we have

$$\alpha_{t+1} \leq \frac{\nu + C}{\hat{t} + 1} - \frac{C}{(\hat{t} - 2)(\hat{t} + 1)} + \frac{C}{(\hat{t} + 2)(\hat{t} + 1)} \leq \frac{\nu + C}{\hat{t} + 1}.$$

This proves (44). To get a bound on the distance to the minima x^* , we then have

$$\begin{aligned} \mathbb{E}[\|x_t - x^*\|^2] &\leq 2\mathbb{E}[\|x_t - x_t^*\|^2] + 2\|x_t^* - x^*\|^2 \\ &\leq \frac{2(\nu + C)}{\hat{t}} + 2\|x_t^* - x^*\|^2. \end{aligned}$$

We can again use Corollary 22, letting $\gamma_1 = 0, \gamma_2 = \gamma_t$ in the statement of that result. We then get

$$\|x_t^* - x^*\| \leq \frac{C\kappa^2}{\hat{t}^2} \leq \frac{C}{\hat{t}}.$$

This again uses the fact that $\kappa^2 \leq b \leq \hat{t}$. Combining, this implies

$$\mathbb{E}[\|x_t - x^*\|^2] \leq \frac{2\nu}{\hat{t}} + \frac{4C}{\hat{t}}.$$

Substituting in C , this proves the desired result. ■

Appendix C. Datasets and Models

Below, we provide detailed description of the datasets and models used in the paper. We use federated versions of vision datasets FEMNIST (Caldas et al., 2018) and CIFAR-100 (Krizhevsky and Hinton, 2009), and language modeling datasets Shakespeare (McMahan et al., 2017) and StackOverflow (Authors, 2019). We give descriptions of the datasets, models, and tasks below.

CIFAR-100 The CIFAR-100 dataset is a popular computer vision dataset consisting of $32 \times 32 \times 3$ images with 100 possible labels. While this dataset is not a federated dataset, a federated version was created by Reddi et al. (2020), using hierarchical latent Dirichlet allocation to enforce moderate amounts of heterogeneity among clients. The resulting dataset has 500 clients, each with 100 unique examples. We train a ResNet-18 on this dataset, where we replace all batch normalization layers with group normalization layers (Wu and He, 2018). The use of group norm over batch norm in federated learning was first advocated by Hsieh et al. (2019).

We perform small amounts of data augmentation and preprocessing, as is standard with CIFAR-100. We first perform a random crop to shape $(24, 24, 3)$, followed by a random horizontal flip. We then normalize the pixel values according to their mean and standard deviation. Thus, given an image x , we compute $(x - \mu)/\sigma$ where μ is the average of the pixel values in x , and σ is the standard deviation.

FEMNIST FEMNIST consists of 28×28 gray-scale images of both numbers and upper- and lower-case English characters, with 62 possible labels in total. The digits are partitioned according to their author, resulting in a naturally heterogeneous federated dataset. We do not use any preprocessing on the images. We train a moderately-sized CNN, with identical architecture to the CNN used by McMahan et al. (2017). The CNN contains two convolutional layers, each with 5×5 kernels. The convolutional layers have 32 and 64 filters, respectively, and are each followed by a 2×2 max pooling layer. Finally, the model has a dense layer with 512 units and ReLU activation, followed by a softmax activation.

Shakespeare The Shakespeare dataset is derived from the benchmark designed by Caldas et al. (2018). The dataset corpus is the collected works of William Shakespeare, and the clients correspond to roles in Shakespeare’s plays with at least two lines of dialogue. To eliminate confusion, *character* here will refer to alphanumeric and other such symbols, while we will use *client* to denote the various roles in plays. We split each client’s lines into sequences of 80 characters, padding if necessary. We use a vocabulary size of 90: 86 characters contained in Shakespeare’s work, beginning and end of line tokens, padding tokens, and out-of-vocabulary tokens. We perform next-character prediction on the clients’ dialogue using an RNN. The RNN takes as input a sequence of 80 characters, embeds it into a learned 8-dimensional space, and passes the embedding through 2 LSTM layers, each with 256 units. Finally, we use a softmax output layer with 80 units, where we try to predict a sequence of 80 characters formed by shifting the input sequence over by one. Therefore, our output dimension is 80×90 . We compute loss using cross-entropy loss.

Stack Overflow Stack Overflow is a text datasets consisting of questions and answers posted to the Stack Overflow website. Each user is a client, and their datasets consist of questions and answers posted by this user. Each post has associated meta-data, including a list of associated tags (e.g. a post could have the tag *javascript* if it concerns the javascript language). We perform two tasks on this dataset: tag prediction, and next word prediction. In both cases, we restrict to the 10,000 most frequently used words in the total dataset, as well as the 500 most frequently used tags for the tag prediction task.

For Stack Overflow tag prediction, we use a multi-class logistic regression classifier with 500 output units (one for each of the 500 most frequently used tags), and adopt a one-versus-rest classification strategy. Note that the corresponding multi-class logistic loss is convex.

The inputs to our model are 10,000-dimensional vectors forming bag-of-words vectors for each post. Each vector is normalized to have sum 1.

For Stack Overflow next word prediction, we restrict each client to the first 128 posts in their history (for computational efficiency reasons, as some clients have tens of thousands of posts). We perform truncation and padding so that each post has 21 words (including word tokens for beginning of sentence, end of sentence, padding, and out-of-vocabulary words). The sequence is split into input and output length-20 sequences, corresponding to the first and the last 20 characters (ie. one is the other sequence, shifted by one). The first of these sequences is embedded into a learned 96-dimensional space, and then fed into an LSTM with 670 units. Finally, the output is fed into a densely connected softmax layer with 10,004 units (corresponding to the 10,000 in-vocabulary words, and the extra tokens mentioned above). We attempt to predict the shifted-by-one sequence, and compute the loss via cross-entropy.

Appendix D. Tuned Server Learning Rates

In this section, we detail the best server learning rate η found for each corresponding client learning rate γ and task.

Table 3: Best server learning rate η for each client learning rate γ in the CIFAR-100 task.

| γ | η |
|-----------|-------------|
| 1 | 10^{-1} |
| 10^{-1} | 10^{-1} |
| 10^{-2} | $10^{-3/2}$ |
| 10^{-3} | $10^{-3/2}$ |
| 0 | $10^{-3/2}$ |

Table 4: Best server learning rate η for each client learning rate γ in the FEMNIST task.

| γ | η |
|-----------|-------------|
| 10^{-1} | 10^{-2} |
| 10^{-2} | $10^{-3/2}$ |
| 10^{-3} | $10^{-3/2}$ |
| 0 | $10^{-3/2}$ |

Table 5: Best server learning rate η for each client learning rate γ in the Shakespeare task.

| γ | η |
|-----------|-------------|
| 1 | $10^{-1/2}$ |
| 10^{-1} | 1 |
| 10^{-2} | 10^{-1} |
| 10^{-3} | 10^{-1} |
| 0 | 10^{-1} |

Table 6: Best server learning rate η for each client learning rate γ in the Stack Overflow next word prediction task.

| γ | η |
|-----------|-------------|
| 10^{-1} | $10^{-3/2}$ |
| 10^{-2} | $10^{-3/2}$ |
| 10^{-3} | 10^{-2} |
| 0 | 10^{-2} |

Table 7: Best server learning rate η for each client learning rate γ in the Stack Overflow tag prediction task.

| γ | η |
|-----------|-------------|
| 100 | $10^{-1/2}$ |
| 10 | $10^{-1/2}$ |
| 1 | $10^{-1/2}$ |
| 10^{-1} | $10^{-1/2}$ |
| 10^{-2} | $10^{-1/2}$ |
| 0 | $10^{-1/2}$ |

References

- Antreas Antoniou, Harrison Edwards, and Amos Storkey. How to train your MAML. In *International Conference on Learning Representations*, 2019. URL <https://openreview.net/forum?id=HJGven05Y7>.
- Sean Augenstein, H. Brendan McMahan, Daniel Ramage, Swaroop Ramaswamy, Peter Kairouz, Mingqing Chen, Rajiv Mathews, and Blaise Aguera y Arcas. Generative models for effective ML on private, decentralized datasets. In *International Conference on Learning Representations*, 2020. URL <https://openreview.net/forum?id=SJgaRA4FPH>.
- The TensorFlow Federated Authors. TensorFlow Federated Stack Overflow dataset, 2019. URL https://www.tensorflow.org/federated/api_docs/python/tff/simulation/datasets/stackoverflow/load_data.
- Eugene Bagdasaryan, Andreas Veit, Yiqing Hua, Deborah Estrin, and Vitaly Shmatikov. How to backdoor federated learning. *arXiv preprint arXiv:1807.00459*, 2018.
- Debraj Basu, Deepesh Data, Can Karakus, and Suhas Diggavi. Qsparse-local-SGD: Distributed SGD with quantization, sparsification and local computations. In *Advances in Neural Information Processing Systems*, pages 14668–14679, 2019.
- Keith Bonawitz, Hubert Eichner, Wolfgang Grieskamp, Dzmitry Huba, Alex Ingerman, Vladimir Ivanov, Chloé Kiddon, Jakub Konečný, Stefano Mazzocchi, Brendan McMahan, Timon Van Overveldt, David Petrou, Daniel Ramage, and Jason Roselander. Towards federated learning at scale: System design. In *Proceedings of Machine Learning and Systems 2019*, pages 374–388. 2019.
- Léon Bottou, Frank E Curtis, and Jorge Nocedal. Optimization methods for large-scale machine learning. *Siam Review*, 60(2):223–311, 2018.
- Theodora S Brisimi, Ruidi Chen, Theofanie Mela, Alex Olshevsky, Ioannis Ch Paschalidis, and Wei Shi. Federated learning of predictive models from federated electronic health records. *International journal of medical informatics*, 112:59–67, 2018.
- Sébastien Bubeck. Convex optimization: Algorithms and complexity. *Foundations and Trends in Machine Learning*, 2017.
- Sebastian Caldas, Peter Wu, Tian Li, Jakub Konečný, H Brendan McMahan, Virginia Smith, and Ameet Talwalkar. LEAF: A benchmark for federated settings. *arXiv preprint arXiv:1812.01097*, 2018.
- Mingqing Chen, Ananda Theertha Suresh, Rajiv Mathews, Adeline Wong, Cyril Allauzen, Françoise Beaufays, and Michael Riley. Federated learning of n-gram language models. *arXiv preprint arXiv:1910.03432*, 2019.
- Alireza Fallah, Aryan Mokhtari, and Asuman Ozdaglar. On the convergence theory of gradient-based model-agnostic meta-learning algorithms. *arXiv preprint arXiv:1908.10400*, 2019.

- Alireza Fallah, Aryan Mokhtari, and Asuman Ozdaglar. Personalized federated learning: A meta-learning approach. *arXiv preprint arXiv:2002.07948*, 2020.
- Chelsea Finn, Pieter Abbeel, and Sergey Levine. Model-agnostic meta-learning for fast adaptation of deep networks. In *Proceedings of the 34th International Conference on Machine Learning-Volume 70*, pages 1126–1135. JMLR, 2017.
- Avishek Ghosh, Justin Hong, Dong Yin, and Kannan Ramchandran. Robust federated learning in a heterogeneous environment. *arXiv preprint arXiv:1906.06629*, 2019.
- Priya Goyal, Piotr Dollár, Ross Girshick, Pieter Noordhuis, Lukasz Wesolowski, Aapo Kyrola, Andrew Tulloch, Yangqing Jia, and Kaiming He. Accurate, large minibatch SGD: Training ImageNet in 1 hour. *arXiv preprint arXiv:1706.02677*, 2017.
- Erin Grant, Chelsea Finn, Sergey Levine, Trevor Darrell, and Thomas Griffiths. Recasting gradient-based meta-learning as hierarchical Bayes. In *International Conference on Learning Representations*, 2018. URL https://openreview.net/forum?id=BJ_UL-k0b.
- Theodore Groves and Thomas Rothenberg. A note on the expected value of an inverse matrix. *Biometrika*, 56(3):690–691, 1969.
- Andrew Hard, Kanishka Rao, Rajiv Mathews, Swaroop Ramaswamy, Françoise Beaufays, Sean Augenstein, Hubert Eichner, Chloé Kiddon, and Daniel Ramage. Federated learning for mobile keyboard prediction. *arXiv preprint arXiv:1811.03604*, 2018.
- Andrew Hard, Kurt Partridge, Cameron Nguyen, Niranjan Subrahmanya, Aishanee Shah, Pai Zhu, Ignacio Lopez Moreno, and Rajiv Mathews. Training keyword spotting models on non-IID data with federated learning. *arXiv preprint arXiv:2005.10406*, 2020.
- Kevin Hsieh, Amar Phanishayee, Onur Mutlu, and Phillip B Gibbons. The non-IID data quagmire of decentralized machine learning. *arXiv preprint arXiv:1910.00189*, 2019.
- Tzu-Ming Harry Hsu, Hang Qi, and Matthew Brown. Measuring the effects of non-identical data distribution for federated visual classification. *arXiv preprint arXiv:1909.06335*, 2019.
- Alex Ingerman and Krzys Ostrowski. Introducing tensorflow federated, 2019. URL <https://medium.com/tensorflow/introducing-tensorflow-federated-a4147aa20041>.
- Yihan Jiang, Jakub Konečný, Keith Rush, and Sreeram Kannan. Improving federated learning personalization via model agnostic meta learning. *arXiv preprint arXiv:1909.12488*, 2019.
- Peter Kairouz, H Brendan McMahan, Brendan Avent, Aurélien Bellet, Mehdi Bennis, Arjun Nitin Bhagoji, Keith Bonawitz, Zachary Charles, Graham Cormode, Rachel Cummings, et al. Advances and open problems in federated learning. *arXiv preprint arXiv:1912.04977*, 2019.
- Sai Praneeth Karimireddy, Satyen Kale, Mehryar Mohri, Sashank J Reddi, Sebastian U Stich, and Ananda Theertha Suresh. SCAFFOLD: Stochastic controlled averaging for on-device federated learning. *arXiv preprint arXiv:1910.06378*, 2019.

- A Khaled, K Mishchenko, and P Richtárik. Tighter theory for local SGD on identical and heterogeneous data. In *The 23rd International Conference on Artificial Intelligence and Statistics (AISTATS 2020)*, 2020.
- Mikhail Khodak, Maria-Florina F Balcan, and Ameet S Talwalkar. Adaptive gradient-based meta-learning methods. In *Advances in Neural Information Processing Systems*, pages 5915–5926, 2019.
- Diederik P Kingma and Jimmy Ba. Adam: A method for stochastic optimization. *arXiv preprint arXiv:1412.6980*, 2014.
- Jakub Konečný, H Brendan McMahan, Felix X Yu, Peter Richtárik, Ananda Theertha Suresh, and Dave Bacon. Federated learning: Strategies for improving communication efficiency. *arXiv preprint arXiv:1610.05492*, 2016.
- Alex Krizhevsky. One weird trick for parallelizing convolutional neural networks. *arXiv preprint arXiv:1404.5997*, 2014.
- Alex Krizhevsky and Geoffrey Hinton. Learning multiple layers of features from tiny images. Technical report, Citeseer, 2009.
- Tian Li, Anit Kumar Sahu, Ameet Talwalkar, and Virginia Smith. Federated learning: Challenges, methods, and future directions. *arXiv preprint arXiv:1908.07873*, 2019.
- Tian Li, Anit Kumar Sahu, Manzil Zaheer, Maziar Sanjabi, Ameet Talwalkar, and Virginia Smith. Federated optimization in heterogeneous networks. In *Proceedings of Machine Learning and Systems 2020*, pages 429–450. 2020a.
- Tian Li, Maziar Sanjabi, Ahmad Beirami, and Virginia Smith. Fair resource allocation in federated learning. In *International Conference on Learning Representations*, 2020b. URL <https://openreview.net/forum?id=ByexELSYDr>.
- Xiang Li, Kaixuan Huang, Wenhao Yang, Shusen Wang, and Zhihua Zhang. On the convergence of fedavg on non-IID data. In *International Conference on Learning Representations*, 2020c. URL <https://openreview.net/forum?id=HJxNAnVtDS>.
- Grigory Malinovsky, Dmitry Kovalev, Elnur Gasanov, Laurent Condat, and Peter Richtarik. From local SGD to local fixed point methods for federated learning. *arXiv preprint arXiv:2004.01442*, 2020.
- Brendan McMahan, Eider Moore, Daniel Ramage, Seth Hampson, and Blaise Agüera y Arcas. Communication-efficient learning of deep networks from decentralized data. In *Proceedings of the 20th International Conference on Artificial Intelligence and Statistics, AISTATS 2017*, pages 1273–1282, 2017.
- H. Brendan McMahan, Daniel Ramage, Kunal Talwar, and Li Zhang. Learning differentially private recurrent language models. In *International Conference on Learning Representations*, 2018. URL <https://openreview.net/forum?id=BJ0hF1Z0b>.

- Mehryar Mohri, Gary Sivek, and Ananda Theertha Suresh. Agnostic federated learning. *arXiv preprint arXiv:1902.00146*, 2019.
- Alex Nichol, Joshua Achiam, and John Schulman. On first-order meta-learning algorithms. *arXiv preprint arXiv:1803.02999*, 2018.
- Reese Pathak and Martin J Wainwright. FedSplit: An algorithmic framework for fast federated optimization. *arXiv preprint arXiv:2005.05238*, 2020.
- Aniruddh Raghu, Maithra Raghu, Samy Bengio, and Oriol Vinyals. Rapid learning or feature reuse? towards understanding the effectiveness of MAML. In *International Conference on Learning Representations*, 2020. URL <https://openreview.net/forum?id=rkgMkCEtPB>.
- Aravind Rajeswaran, Chelsea Finn, Sham M Kakade, and Sergey Levine. Meta-learning with implicit gradients. In *Advances in Neural Information Processing Systems*, pages 113–124, 2019.
- Alexander Rakhlin, Ohad Shamir, and Karthik Sridharan. Making gradient descent optimal for strongly convex stochastic optimization. In *Proceedings of the 29th International Conference on Machine Learning (ICML-12)*, pages 449–456, 2012.
- Sashank Reddi, Zachary Charles, Manzil Zaheer, Zachary Garrett, Keith Rush, Jakub Konečný, Sanjiv Kumar, and H Brendan McMahan. Adaptive federated optimization. *arXiv preprint arXiv:2003.00295*, 2020.
- Amirhossein Reisizadeh, Aryan Mokhtari, Hamed Hassani, Ali Jadbabaie, and Ramtin Pedarsani. FedPAQ: A communication-efficient federated learning method with periodic averaging and quantization. In *The 23rd International Conference on Artificial Intelligence and Statistics (AISTATS 2020)*, 2020.
- Andrei A. Rusu, Dushyant Rao, Jakub Sygnowski, Oriol Vinyals, Razvan Pascanu, Simon Osindero, and Raia Hadsell. Meta-learning with latent embedding optimization. In *International Conference on Learning Representations*, 2019. URL <https://openreview.net/forum?id=BJgklhAcK7>.
- Sumudu Samarakoon, Mehdi Bennis, Walid Saad, and Merouane Debbah. Federated learning for ultra-reliable low-latency V2V communications. In *2018 IEEE Global Communications Conference (GLOBECOM)*, pages 1–7. IEEE, 2018.
- Felix Sattler, Simon Wiedemann, Klaus-Robert Müller, and Wojciech Samek. Robust and communication-efficient federated learning from non-IID data. *IEEE transactions on neural networks and learning systems*, 2019.
- Sebastian U. Stich. Local SGD converges fast and communicates little. In *International Conference on Learning Representations*, 2019. URL <https://openreview.net/forum?id=S1g2JnRcFX>.
- Sebastian U Stich and Sai Praneeth Karimireddy. The error-feedback framework: Better rates for SGD with delayed gradients and compressed communication. *arXiv preprint arXiv:1909.05350*, 2019.

- Ziteng Sun, Peter Kairouz, Ananda Theertha Suresh, and H Brendan McMahan. Can you really backdoor federated learning? *arXiv preprint arXiv:1911.07963*, 2019.
- Joaquin Vanschoren. Meta-learning. In *Automated Machine Learning*, pages 35–61. Springer, 2019.
- Jianyu Wang and Gauri Joshi. Cooperative SGD: A unified framework for the design and analysis of communication-efficient SGD algorithms. *arXiv preprint arXiv:1808.07576*, 2018.
- Yuhong Wen, Wenqi Li, Holger Roth, and Prerna Dogra. Federated learning powered by NVIDIA Clara, December 2019. URL <https://devblogs.nvidia.com/federated-learning-clara/>. NVIDIA Developer Blog.
- Blake Woodworth, Kumar Kshitij Patel, Sebastian U Stich, Zhen Dai, Brian Bullins, H Brendan McMahan, Ohad Shamir, and Nathan Srebro. Is local SGD better than minibatch SGD? *arXiv preprint arXiv:2002.07839*, 2020.
- Yuxin Wu and Kaiming He. Group normalization. In *Proceedings of the European Conference on Computer Vision (ECCV)*, pages 3–19, 2018.
- Cong Xie, Oluwasanmi Koyejo, Indranil Gupta, and Haibin Lin. Local AdaAlter: Communication-efficient stochastic gradient descent with adaptive learning rates. *arXiv preprint arXiv:1911.09030*, 2019.
- Qiang Yang, Yang Liu, Tianjian Chen, and Yongxin Tong. Federated machine learning: Concept and applications. *ACM Transactions on Intelligent Systems and Technology (TIST)*, 10(2):1–19, 2019.
- Timothy Yang, Galen Andrew, Hubert Eichner, Haicheng Sun, Wei Li, Nicholas Kong, Daniel Ramage, and Françoise Beaufays. Applied federated learning: Improving google keyboard query suggestions. *arXiv preprint arXiv:1812.02903*, 2018.
- Hao Yu, Sen Yang, and Shenghuo Zhu. Parallel restarted SGD with faster convergence and less communication: Demystifying why model averaging works for deep learning. In *Proceedings of the AAAI Conference on Artificial Intelligence*, volume 33, pages 5693–5700, 2019.
- Manzil Zaheer, Sashank Reddi, Devendra Sachan, Satyen Kale, and Sanjiv Kumar. Adaptive methods for nonconvex optimization. In *Advances in Neural Information Processing Systems*, pages 9815–9825, 2018.
- Michael Zhang, James Lucas, Jimmy Ba, and Geoffrey E Hinton. Lookahead optimizer: k steps forward, 1 step back. In *Advances in Neural Information Processing Systems*, pages 9593–9604, 2019.
- Martin Zinkevich, Markus Weimer, Lihong Li, and Alex J Smola. Parallelized stochastic gradient descent. In *Advances in neural information processing systems*, pages 2595–2603, 2010.